Modelling of Sloshing in Free Surface Tanks for ShipMo3D Ship Motion Predictions

Kevin McTaggart

Prepared for:

Canadian Coast Guard Major Crown Projects Directorate
Ottawa

Defence Research and Development Canada – Atlantic
External Client Report
DRDC Atlantic ECR 2011-084
January 2012

Abstract

Ship roll motions in waves can be significantly influenced by the presence of tanks containing liquids, which experience sloshing. Sloshing effects must be considered when transporting liquid cargo; however, sloshing can also be used to advantage. Many vessels have specially designed flume tanks to provide passive roll stabilization. This report describes the implementation of a model of fluid sloshing in tanks for the ShipMo3D ship motion library. The sloshing model is based on potential flow, giving a solution that is computationally efficient and robust. The potential flow model includes a simplified treatment of flow damping arising from viscous effects. The tank sloshing model has been implemented for computations in both the frequency and time domains. Example computations for a generic frigate demonstrate the reduction of roll motions using a flume tank.

Résumé

Le mouvement de roulis des navires peut être considérablement influencé par la présence de citernes renfermant des liquides qui sont assujettis au ballottement. Il est important de tenir compte de l'effet de ballottement lors du transport de cargaisons contenant des liquides. Cependant, il est également possible d'en tirer parti. Bon nombre de bâtiments sont en effet munis de citernes antiroulis spécialement conçues pour assurer la stabilisation passive dans la houle. Le présent rapport décrit la mise en œuvre d'un modèle du ballottement des fluides contenus dans des citernes servant à enrichir la bibliothèque de données sur les mouvements de navires du logiciel ShipMo3D. Le modèle de ballottement est basé sur l'écoulement potentiel et offre des solutions efficaces et fiables sur le plan des calculs. Le modèle basé sur l'écoulement potentiel comprend un traitement simplifié de l'amortissement de l'écoulement dû à la viscosité. Le modèle du ballottement en citerne a été mis en œuvre pour effectuer des calculs dans le domaine temporel et le domaine fréquentiel. Des exemples de calculs pour une frégate générique démontrent la réduction du roulis lorsque l'on utilise une citerne antiroulis.

This page intentionally left blank.

Executive summary

Modelling of Sloshing in Free Surface Tanks for ShipMo3D Ship Motion Predictions

Kevin McTaggart; DRDC Atlantic ECR 2011-084; Defence Research and Development Canada – Atlantic; January 2012.

Introduction: Ship roll motions in waves can be significantly influenced by the presence of tanks containing liquids, which experience sloshing. Sloshing effects must be considered when transporting liquid cargo; however, sloshing can also be used to advantage. Many vessels have specially designed flume tanks to provide passive roll stabilization. Flume tank dimensions can be designed to provide optimal reduction of roll motions. In comparison to other roll stabilization methods, flume tanks (and U-tube tanks) have the advantages of being effective at zero ship speed and being protected from environmental hazards such as ice.

Principal Results: This report describes the implementation of a model of fluid sloshing in tanks for the ShipMo3D ship motion library. The sloshing model is based on potential flow, giving a solution that is computationally efficient and robust. The potential flow model includes a simplified treatment of flow damping arising from viscous effects. The tank sloshing model has been implemented for computations in both the frequency and time domains. Numerical roll predictions for a barge model with sloshing tanks show good agreement with experimental results. Example computations for a generic frigate demonstrate the reduction of roll motions using a flume tank. The sloshing tank capability has been integrated into ShipMo3D Version 3.0.

Significance of Results: The ShipMo3D ship motion library can now be used to assess the influence of tank sloshing on ship motions. This capability can be used to design flume tanks for roll stabilization. The potential flow model of sloshing is suitable for analysis of a ship with moderate motion amplitudes. Due to the complex nature of sloshing phenomena, it is recommended that predicted results be compared with other approaches, such as model tests or computational fluid dynamics.

Future Plans: Future work will likely investigate more sophisticated models of tank sloshing, including large amplitude motions and more detailed treatment of viscous effects.

Sommaire

Modelling of Sloshing in Free Surface Tanks for ShipMo3D Ship Motion Predictions

Kevin McTaggart ; DRDC Atlantic ECR 2011-084 ; Recherche et développement pour la défense Canada – Atlantique ; janvier 2012.

Introduction : Le mouvement de roulis des navires peut être considérablement influencé par la présence de citernes renfermant des liquides qui sont assujettis au ballottement. Il est important de tenir compte de l'effet de ballottement lors du transport de cargaisons contenant des liquides. Cependant, il est également possible d'en tirer parti. Bon nombre de bâtiments sont en effet munis de citernes antiroulis spécialement conçues pour assurer la stabilisation passive dans la houle. Les dimensions des citernes antiroulis peuvent être conçues de manière à réduire le plus possible les effets du roulis. Comparativement à d'autres méthodes de stabilisation, les citernes antiroulis (et les citernes à tube en U) ont l'avantage d'être efficaces même lorsque le navire est à l'arrêt, et sont protégées contre les dangers associés à certaines conditions environnementales, comme la glace.

Résultats principaux : Le présent rapport décrit la mise en œuvre d'un modèle du ballottement des fluides contenus dans des citernes servant à enrichir la bibliothèque de données sur le mouvement des navires du logiciel ShipMo3D. Le modèle de ballottement est basé sur l'écoulement potentiel et offre des solutions efficaces et fiables sur le plan des calculs. Le modèle basé sur l'écoulement potentiel comprend un traitement simplifié de l'amortissement de l'écoulement dû à la viscosité. Le modèle du ballottement en citerne a été mis en œuvre pour effectuer des calculs dans le domaine temporel et le domaine fréquentiel. Les prévisions numériques du roulis pour un modèle de barge doté de citernes antiroulis font état d'une bonne concordance avec les résultats expérimentaux. Des exemples de calculs pour une frégate générique démontrent la réduction du roulis lorsque l'on utilise une citerne antiroulis.

Importance des résultats : La bibliothèque de données du logiciel ShipMo3D sur le mouvement des navires peut maintenant être utilisée pour évaluer l'effet des citernes antiroulis sur le mouvement des navires. Cette capacité peut être utilisée pour concevoir des citernes antiroulis assurant la stabilisation dans la houle. Le modèle d'écoulement potentiel pour le ballottement convient à l'analyse du mouvement à amplitude modérée d'un navire. En raison de la complexité du phénomène de ballottement, il est recommandé que les résultats prévus soient comparés à d'autres approches, comme les essais de modèles ou la dynamique des fluides numérique.

Travaux ultérieurs prévus : Les recherches futures porteront vraisemblablement sur des modèles perfectionnés du ballottement en citerne, y compris des mouvements de navires à grande amplitude et sur un traitement plus approfondi des effets de la viscosité.

Table of contents

List of tables

List of figures

This page intentionally left blank.

1 Introduction

Ship motions in waves affect the performance of both humans and ship systems. If a ship is carrying tanks filled with liquid, then sloshing can occur and influence ship motion. The influence of sloshing can be especially important for roll motions. On many ships, sloshing is used to advantage through passive flume tanks that are designed to minimize ship roll motions. In comparison with other roll stabilization methods, roll stabilization tanks (including both flume tanks and U-tube tanks) have the advantages of being effective at all ship speeds. Furthermore, roll stabilization tanks are rugged and can be contained within the hull, thus making them protected from ice and other environmental hazards that a ship might encounter.

In anticipation of ongoing design work, the Canadian Coast Guard tasked DRDC Atlantic with adding a capability for modelling sloshing tanks with free surfaces in the ShipMo3D ship motion library. Modelling of sloshing has been implemented in both the frequency and time domains in Version 3 of ShipMo3D [1, 2]. ShipMo3D Version 3 also includes modelling of U-tube tanks [3]. This report describes the implementation of a sloshing model, which can be used for analysis of flume tanks and other tanks carrying liquid onboard a ship. Section 2 gives coordinate systems used for evaluating ship motions in waves. The equations of ship motion including a sloshing tank are given in Section 3. Section 4 describes the sloshing forces relative to an origin at the tank fluid line, and Section 5 describes the resulting forces in the frequency domain acting on the ship. Extension of computations to the time domain is described in Section 6. Parametric studies in Section 7 show sloshing forces for tanks of different geometries and demonstrate convergence of results for different varying input parameters. Section 8 presents validation of roll motion computations using experimental data for a barge. Section 9 gives an example design of a flume tank for roll stabilization of a generic frigate. Discussion of results and application is given in Section 10, followed by final conclusions in Section 11.

2 Coordinate Systems for Ship Motions in Waves and Sloshing Tank

ShipMo3D uses 2 main coordinate systems for evaluating ship motions in waves. Figure 1 shows a translating earth coordinate system, which is used for frequency domain motions and also for evaluating hydrodynamic forces. The translating earth coordinate system moves with the mean forward speed of the ship. Figure 2 shows how relative sea direction is defined in the translating earth coordinate system. For time domain computations, which can involve a freely maneuvering ship, motions are given in the earth-fixed coordinate system of Figure 3. Within ShipMo3D time domain computations, forces and accelerations at each time step are evaluated using a translating earth coordinate system and then converted to the earth-fixed system.

Figure 4 shows the coordinate system for a sloshing tank. When describing tank input geometry in ShipMo3D, the coordinates are given relative to the tank baseline, which is located at elevation z_{bl}^{tank} above the ship baseline. When performing hydrodynamic computations of flow sloshing within ShipMo3D, vertical coordinates z_{fl} are relative to the mean fluid level within the tank. The computed results can then be easily transformed to a specified vertical origin, which is typically the ship vertical centre of gravity. This approach allows the adjustment of the vertical tank location z_{bl}^{tank} without having to re-evaluate the complex sloshing analysis.

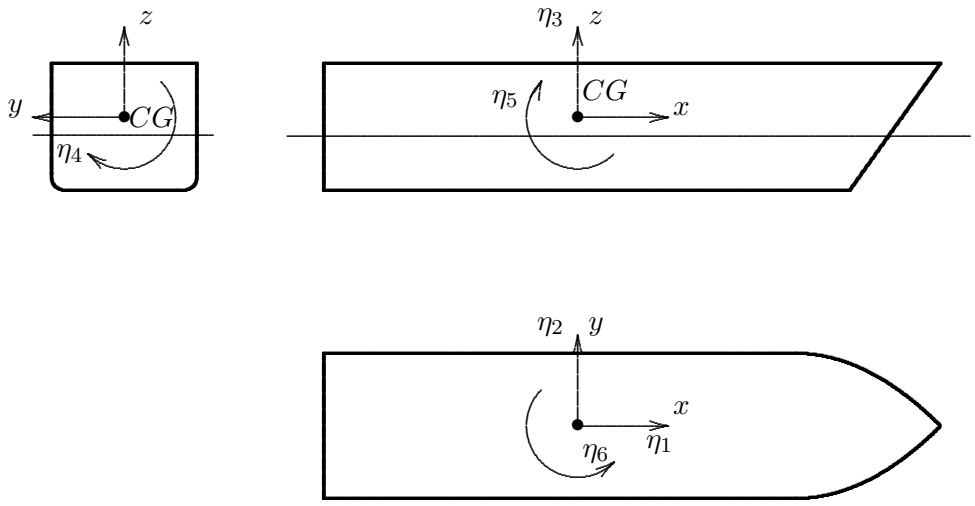

Figure 1: *Translating Earth Coordinate System for Frequency Domain Motions and Solution of Hydrodynamic Forces*

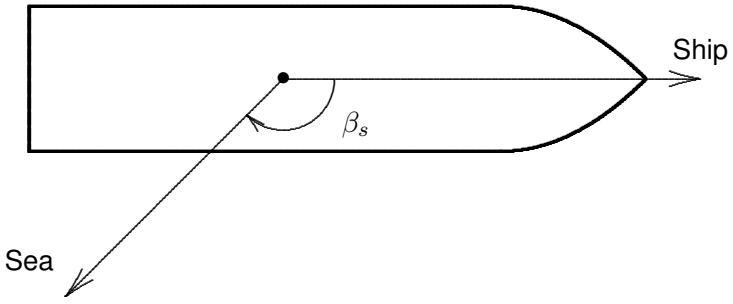

Figure 2: *Relative Sea Direction*

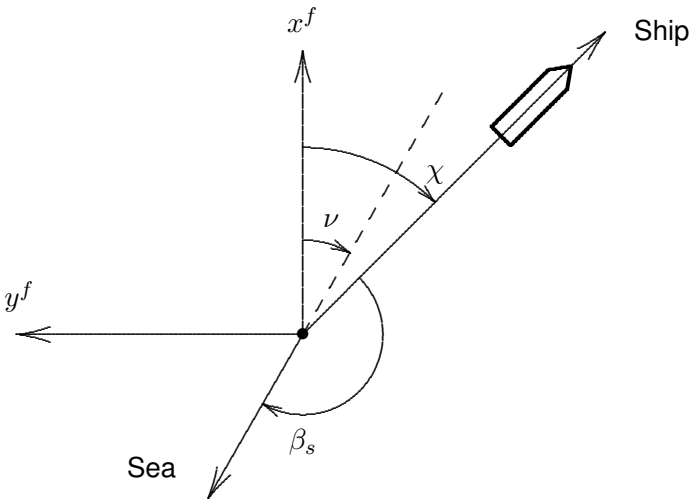

Figure 3: *Earth-Fixed Coordinate System for Time Domain Motions*

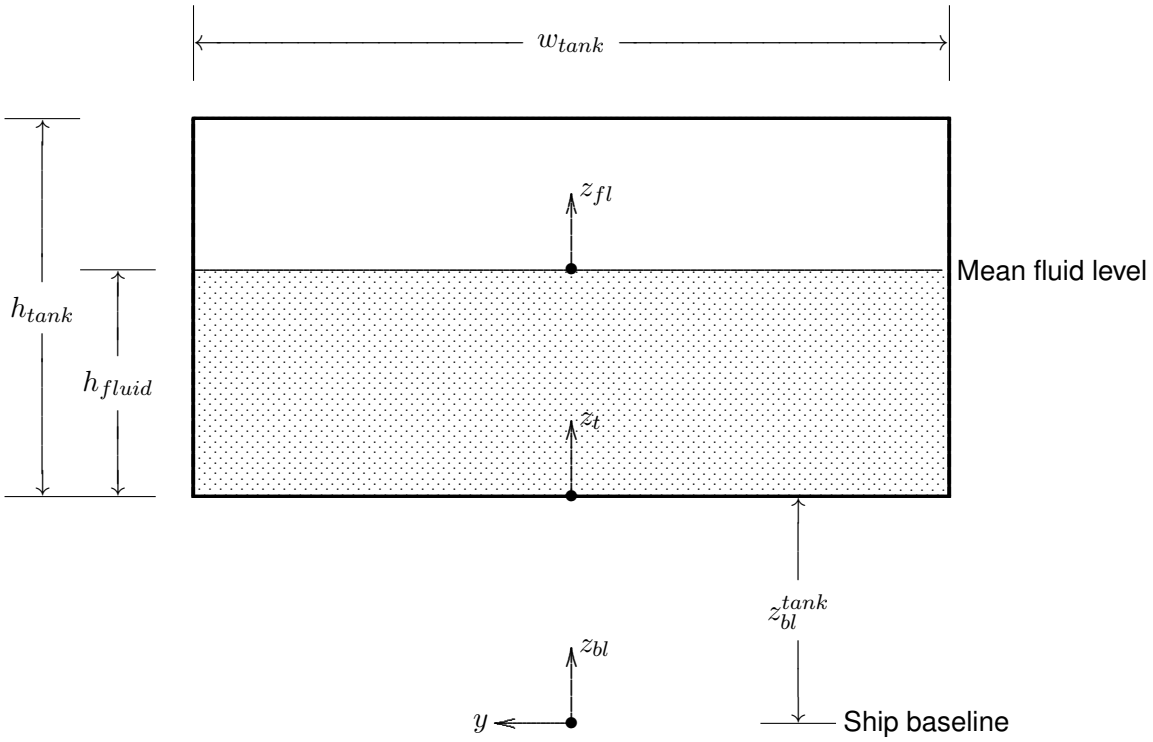

Figure 4: *Tank Coordinate System for Sloshing*

3 Equations of Ship Motion in the Frequency Domain Including Sloshing in a Tank

The extension of ShipMo3D to include tank sloshing is based largely on the work of Malenica et al. [4]. Similar work has been done by Newman [5] and Lee et al. [6]. Unlike the U-tube tank implementation of Reference 3, the sloshing tank analysis does not introduce an extra degree of freedom to the ship motion analysis. Instead, the water sloshing inside a tank is treated similarly to the water outside of the ship, and can be modelled using added mass, damping, and stiffness terms influencing the 6 rigid-body degrees of freedom for the ship. Consequently, the motions of the ship including sloshing can be expressed in the frequency domain as follows:

$$\begin{aligned}\left([M] + [A] + [A^{slosh}]\right)\{\ddot{\eta}\} + \left([B] + [B^{slosh}]\right)\{\dot{\eta}\} \\ + \left([C] + [C^{slosh}]\right)\{\eta\} = \{F_I\} + \{F_D\}\end{aligned} \quad (1)$$

where $[M]$ is the ship inertia matrix, $[A]$ is the ship added mass matrix due to water exterior to the ship, $[A^{slosh}]$ is the added mass matrix due to sloshing inside fluid tanks, $\{\ddot{\eta}\}$ is the ship acceleration vector, $[B]$ is the ship damping matrix due to water exterior to the ship, $[B^{slosh}]$ is the damping matrix due to sloshing inside fluid tanks, $\{\dot{\eta}\}$ is the ship velocity vector, $[C]$ is the ship hydrodynamic stiffness matrix, $[C^{slosh}]$ is the sloshing matrix due to sloshing inside fluid tanks, $\{F_I\}$ is the incident wave force vector, and $\{F_D\}$ is the diffracted wave force vector. For the present discussion, appendages forces and hull viscous forces are not considered. The hull hydrodynamic force terms in Equation (1) are discussed in detail in References 7 and 8.

For treatment of fluid within tanks for ShipMo3D, the mass of tank fluids without sloshing effects is included in the ship mass matrix $[M]$, and the terms $[A^{slosh}]$, $[B^{slosh}]$, and $[C^{slosh}]$ account for the dynamic motion of fluid within tanks. This approach allows for ship displacement and trim to be considered in a conventional manner (i.e., the total ship displacement includes the influence of tank fluid masses within the ship).

4 Evaluation of Tank Hydrodynamic Forces in Frequency Domain for Coordinate System with Vertical Origin at Tank Fluid Line

Evaluation of tank sloshing force terms is performed in two stages. During the first stage, total hydrodynamic forces arising from the tank fluid are evaluated in a coordinate system relative to the tank fluid line (see Figure 4). During the second stage, the tank hydrodynamic forces are converted to the coordinate system with its origin at the ship centre of gravity. Furthermore, the hydrodynamic force terms evaluated during the second stage subtract the static mass of the fluid, leaving only the incremental effect of sloshing. This two stage approach allows for the tank to be moved to different locations on the ship without requiring full re-computation of tank hydrodynamic forces.

The evaluation of tank sloshing forces is very similar to the evaluation of hydrodynamic forces on the exterior of the hull described in Reference 7. The oscillatory ship motions in the time domain are related to the oscillatory ship motions in the frequency domain as follows:

$$\eta_j^{TD}(t) = \eta_j \; e^{i\,\omega_e\,t} \text{ for } j = 1 - 6 \tag{2}$$

where η_j^{TD} is ship displacement in the time domain for mode j, η_j is complex ship motion amplitude in the frequency domain, ω_e is ship motion frequency (equal to wave encounter frequency), and t is time. The velocity potential describing the sloshing flow within the tank is expressed as:

$$\Phi(\vec{x}, t) = \text{Real}\left\{ \left[\sum_{j=1}^{6} \eta_j \; \phi_j(\vec{x}) \right] \; e^{i\,\omega_e\,t} \right\} \tag{3}$$

where Φ is the total velocity potential in the time domain, $\vec{x}$ is the location within the fluid domain, and ϕ_j is the velocity potential in the frequency domain for unit amplitude ship motions in mode j. The complex dynamic pressure within the tank fluid is given by the following in the frequency domain based on Bernoulli's equation:

$$p = -\rho_{tank} \; i \; \omega_e \left[\sum_{j=1}^{6} \eta_j \; \phi_j(\vec{x}) \right] \tag{4}$$

where ρ_{tank} is the tank fluid density. Using the above pressure, added mass and damping terms describing the fluid forces acting on the tank walls are:

$$A_{jk}^{tank-fl} \;\; = \;\; -\frac{\rho_{tank}}{\omega_e} \int_{S_t} \text{Imag}\left(\phi_k\right) \; n_j^{fl} \; dS \tag{5}$$

$$B_{jk}^{tank-fl} \;=\; -\rho_{tank} \int_{S_t} \mathrm{Imag}\,(\phi_k)\; n_j^{fl}\; dS \tag{6}$$

where S_t is the surface of the tank, and n_j^{fl} is the normal vector for each mode j based on the vertical origin at the fluid line. Note that the terms $A^{tank-fl}$ and $B^{tank-fl}$ include the total forces required to move the fluid within the tank (including all inertia forces in the absence of sloshing), and that these terms are evaluated for motions about a vertical axis with origin at the tank fluid level rather than the ship centre of gravity. The normals for each motion mode k are given by:

$$n_1^{fl} \;=\; n_x \tag{7}$$
$$n_2^{fl} \;=\; n_y \tag{8}$$
$$n_3^{fl} \;=\; n_z \tag{9}$$
$$n_4^{fl} \;=\; y\, n_z \;-\; z_{fl}\, n_y \tag{10}$$
$$n_5^{fl} \;=\; z_{fl}\, n_x \;-\; x\, n_z \tag{11}$$
$$n_6^{fl} \;=\; x\, n_y \;-\; y\, n_x \tag{12}$$

where n_x, n_y, and n_z are the directional cosines for the unit normal pointing into the tank fluid. Recall that z_{fl} is the elevation relative to the tank fluid level.

The solutions of the tank fluid velocity potentials ϕ_k must satisfy the continuity equation within the fluid domain and boundary conditions on the tank free surface and tank walls. When solving for potential flow inside a tank, the following boundary can be used used for describing the requirement of zero flow going through tank walls:

$$\frac{\partial \phi_j}{\partial n} \;=\; i\,\omega_e\, n_j^{fl} \text{ on } S_t \text{ for } j = 1-6 \tag{13}$$

The radiated fluid flow for each mode j can be represented by distributing sources of strength σ_j on the inside wetted surface of the tank, with the flow in the fluid domain being expressed by:

$$\phi_j(\vec{x}) \;=\; \frac{1}{4\pi} \int_{S_t} G(\vec{x},\vec{x}_s)\; \sigma_j(\vec{x}_s)\; dS \tag{14}$$

where $\vec{x}$ is the location in the fluid domain, S_t is the wetted surface of the tank, and G is the Green function of flow at $\vec{x}$ arising from a source located at $\vec{x}_s$. The distribution of source strengths σ_j on the wetted surface of the tank are determined by satisfying the flow boundary condition of Equation (13) using the following:

$$-\frac{1}{2}\,\sigma_j(\vec{x}) \;+\; \frac{1}{4\pi} \int_{S_t} \frac{\partial G(\vec{x},\vec{x}_s)}{\partial n_{\vec{x}}}\; \sigma_j(\vec{x}_s)\; dS \;=\; i\,\omega_e\, n_j^{fl}(\vec{x}) \text{ on } S_t \tag{15}$$

The Green function used in the above equation is the frequency domain Green for zero ship forward speed and water of infinite depth described in Reference 7.

The solution presented thus far is based on potential flow, and ignores viscous effects. Malenica et al. [4] present a very useful approach for approximating viscous effects within a sloshing tank. The boundary condition of Equation (13) is modified to include an empirical damping factor ϵ_{tank} as follows:

$$\frac{\partial \phi_j}{\partial n} \;=\; i\,\omega_e\,n_j^{fl} \;+\; \frac{i\,\epsilon_{tank}}{\sqrt[3]{V_{fluid}}}\,\phi_j \text{ on } S_t \text{ for } j = 1-6 \tag{16}$$

The present damping factor is different from that used by Malenica et al., with the fluid volume $V_{fluid}^{1/3}$ being used here for non-dimensionalizing the damping. Selection of $\sqrt[3]{V_{fluid}}$ as a parameter to be used in Equation (16) was based on numerical investigations for various tanks. By using $\sqrt[3]{V_{fluid}}$ in Equation (16), a given value for the damping factor ϵ_{tank} will produce similar results for tanks having varying sizes and geometries. Accounting for the damping factor ϵ_{tank}, Equation (15) for solution of source strengths is modified to the following:

$$-\frac{1}{2}\,\sigma_j(\vec{x}) \;+\; \frac{1}{4\pi}\int_{S_t}\left(\frac{\partial G(\vec{x},\vec{x}_s)}{\partial n_{\vec{x}}} \;-\; \frac{i\,\epsilon_{tank}}{\sqrt[3]{V_{fluid}}}\,G(\vec{x},\vec{x}_s)\right)\,\sigma_j(\vec{x}_s)\,dS$$
$$=\; i\,\omega_e\,n_j^{fl}(\vec{x}) \text{ on } S_t \tag{17}$$

It has been found that good results are obtained when the damping factor ϵ_{tank} is in the range from 0.01 to 0.05. More detailed examination of a suitable damping factor could be performed using physical model tests or computational fluid dynamics (CFD). Within real fluid flow, damping effects are often limited at low and high frequencies, and the following is used to model variation of the damping factor ϵ_{tank} with encounter frequency in the present work:

$$\epsilon_{tank}(\omega_e) \;=\; \left(\frac{\omega_e}{\omega_{lower}^{\hat{\epsilon}}}\right)^2\,\hat{\epsilon}_{tank} \text{ for } \omega_{lower} < \omega_{lower}^{\hat{\epsilon}} \tag{18}$$

$$\epsilon_{tank}(\omega_e) \;=\; \left(\frac{\omega_{upper}^{\hat{\epsilon}}}{\omega_e}\right)^2\,\hat{\epsilon}_{tank} \text{ for } \omega_{upper} > \omega_{upper}^{\hat{\epsilon}} \tag{19}$$

where $\hat{\epsilon}_{tank}$ is the peak value of the damping factor, which is applicable at frequencies ranging from $\omega_{lower}^{\hat{\epsilon}}$ to $\omega_{upper}^{\hat{\epsilon}}$. It is suggested that $\omega_{lower}^{\hat{\epsilon}}$ and $\omega_{upper}^{\hat{\epsilon}}$ be selected such that they encompass the main sloshing frequencies of the tank, which can be determined by examining the variation of added mass with frequency. For sloshing caused by sway motion acting on a box-shaped tank of width w_{tank}, the natural sloshing frequencies are given by [9]:

$$\omega_n^2 \;=\; g\,\lambda_n\,\tanh(\lambda_n\,h_{fluid}) \text{ for } n = 1, 2, \ldots \tag{20}$$

$$\lambda_n \;=\; \frac{n\,\pi}{w_{tank}} \tag{21}$$

where n is the sloshing mode number.

Computations have been performed for a box with length of 4 m, width of 4 m, and fluid height of 2 m. Table 1 show the sloshing natural frequencies for sway based on Equation (20). Figures 5 and 6 show sway added mass and damping coefficients for peak damping coefficient values of 0.0 and 0.05. The sway added mass and damping coefficients show pronounced variations with encounter frequency in the vicinity of the odd numbered sloshing frequencies. The roll added mass and damping coefficients in Figures 7 and 8 show similar behaviour. For the case with zero fluid flow damping $\hat{\epsilon}_{tank} = 0$, the sway and roll added mass coefficients have large ranges of values. For the case with a fluid flow damping value $\hat{\epsilon}_{tank} = 0.05$, the frequency range of maximum damping has been set from a lower frequency $\omega^{\hat{\epsilon}}_{lower}$ of 2 rad/s to an upper frequency $\omega^{\hat{\epsilon}}_{upper}$ of 8 rad/s. The hydrodynamic coefficients computed with $\hat{\epsilon}_{tank} = 0.05$ are likely more realistic than values computed using no fluid flow damping. At the low and high frequency limits, the influence of the fluid flow damping coefficients is negligible.

Table 1: *Sloshing Natural Frequencies for 4 m by 4 m by 2 m Tank Sway Motion*

Mode	Frequency (rad/s)
1	2.658
2	3.917
3	4.806
4	5.550
5	6.205

For surge, sway, and heave motions, the added mass of the tank at zero frequency is equal to the mass of the fluid in the tank because no sloshing occurs. The results in Figure 5 reflect this phenomenon, suggesting that the computations are correct. As discussed by Malenica et al. the added mass in heave at all frequencies is equal to the fluid mass because of the absence of sloshing. As the frequency of the tank motion increases from the zero frequency limit, more complex fluid motion occurs, with the added mass and damping varying with frequency. For the present case of a box with equal length and width, the computed surge coefficients are equal to the computed sway coefficients presented here. For roll, pitch, and yaw motions, the added mass at zero frequency does not typically equal the fluid mass because the acceleration within the fluid can differ from that of a solid mass.

Evaluation of the static mass properties of the fluid in the tank is useful for checking computation, and also for non-dimensionalizing computed added mass and damping

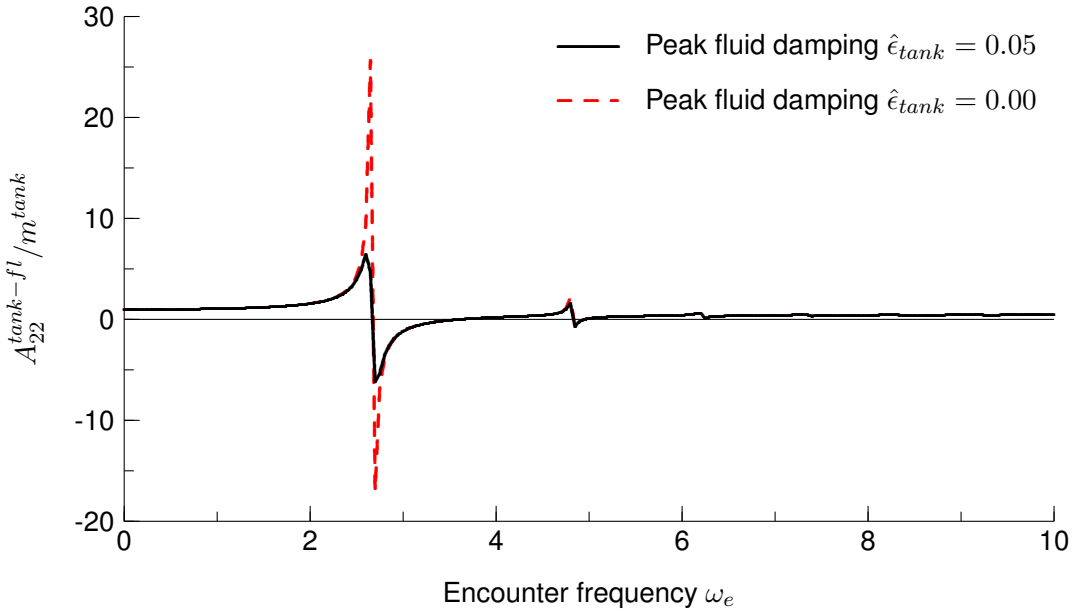

Figure 5: *Sway Added Mass for 4 m by 4 m by 2 m Tank*

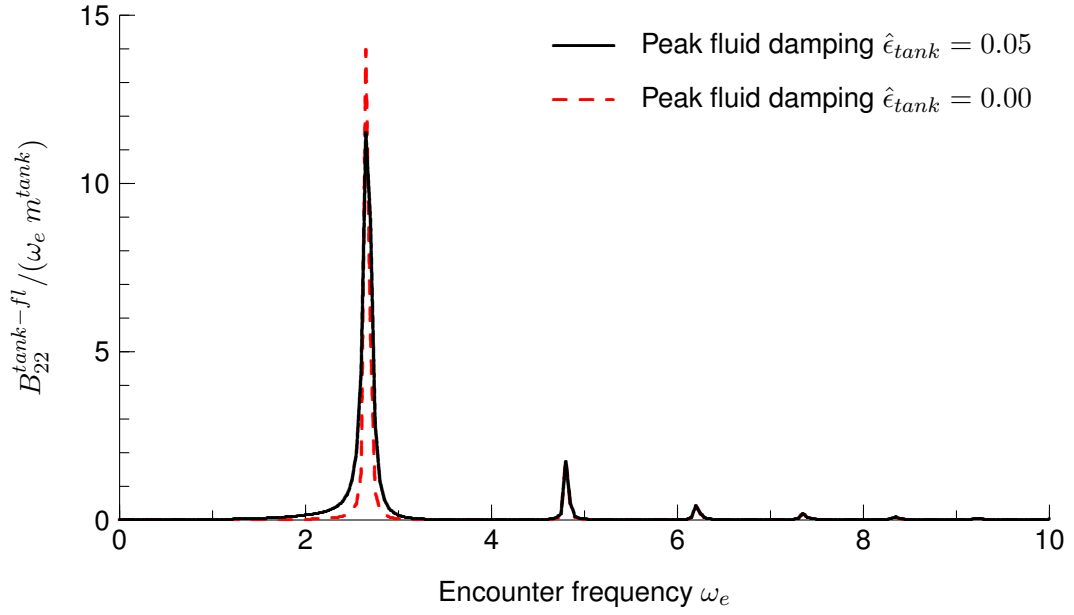

Figure 6: *Sway Damping for 4 m by 4 m by 2 m Tank*

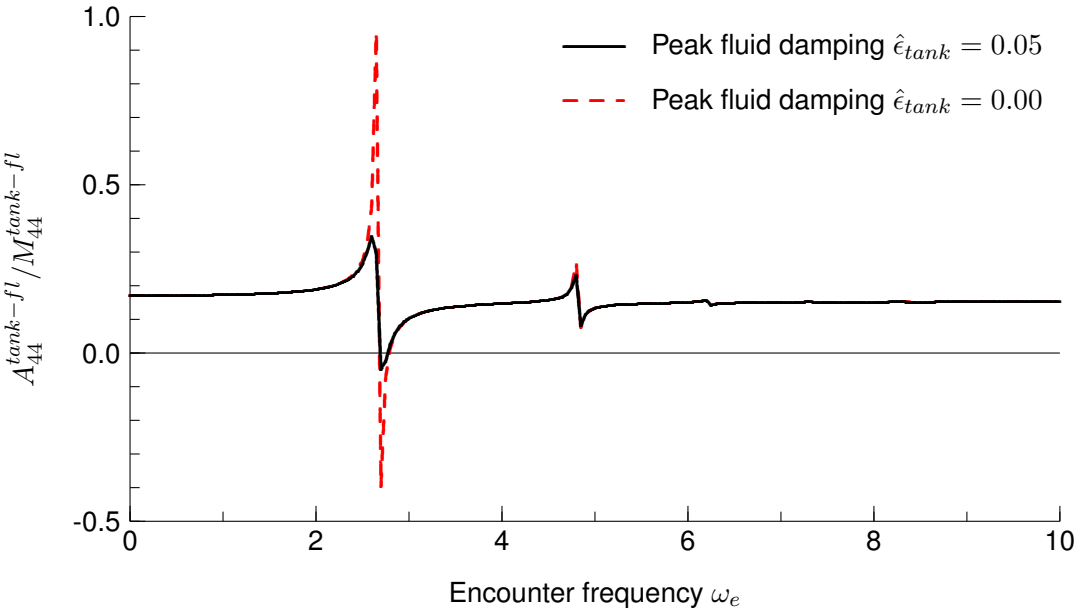

Figure 7: *Roll Added Mass for 4 m by 4 m by 2 m Tank*

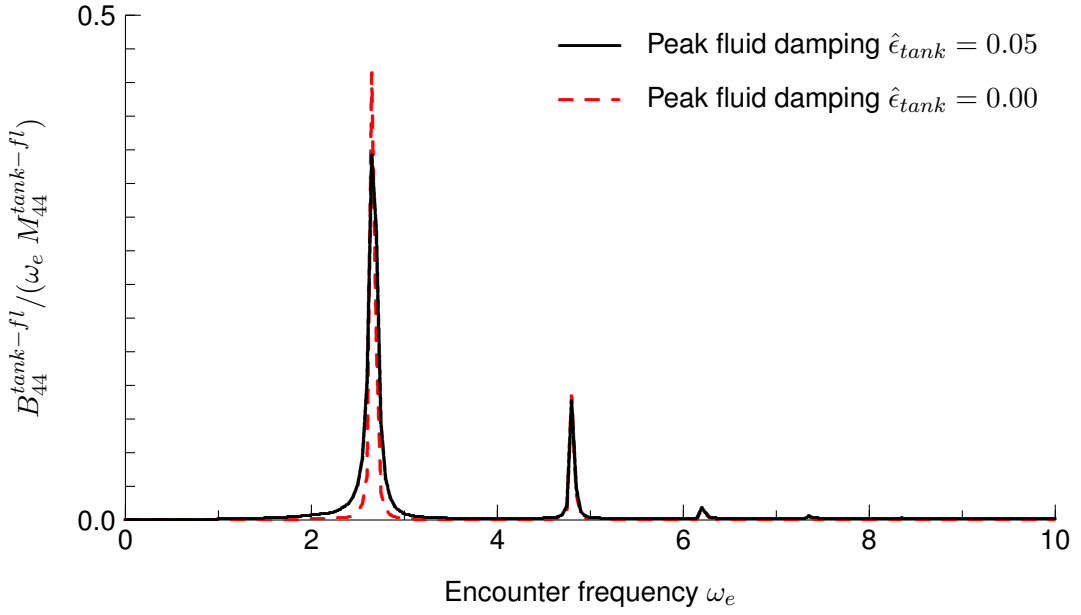

Figure 8: *Roll Damping for 4 m by 4 m by 2 m Tank*

terms. The tank fluid mass matrix $\left[M^{tank-fl}\right]$ is introduced to represent the mass properties of the static fluid in the tank based on the vertical origin at the tank fluid line. The mass of the fluid in the tank is given by:

$$m^{tank} = -\rho_{tank} \int_{S_t} z_{fl}\, n_z\, dS \tag{22}$$

The vertical location of the centroid of mass relative to the fluid line is given by:

$$\overline{z}_{fl}^{tank} = -\frac{1}{m_{tank}}\, \rho_{tank} \int_{S_t} z_{fl}\, y\, n_y\, dS \tag{23}$$

Other required terms can be computed similarly, including the following terms based on x_t and y_t being local tank horizontal coordinates and z_{fl} being elevation relative to the tank fluid line:

$$M_{15}^{tank-fl} = -\frac{1}{2}\, \rho_{tank} \int_{S_t} z_{fl}\, y\, n_y\, dS \tag{24}$$

$$M_{24}^{tank-fl} = \rho_{tank} \int_{S_t} z_{fl}\, x\, n_x\, dS \tag{25}$$

$$M_{26}^{tank-fl} = -\,\rho_{tank} \int_{S_t} x_t\, z_{fl}\, n_z\, dS \tag{26}$$

$$M_{42}^{tank-fl} = M_{24}^{tank-fl} \tag{27}$$

$$M_{44}^{tank-fl} = -\rho_{tank} \int_{S_t} \left(y_t^2 + z_{fl}^2\right) x_t\, n_x\, dS \tag{28}$$

$$M_{46}^{tank-fl} = \rho_{tank} \int_{S_t} x_t\, z_t\, y_t\, n_y\, dS \tag{29}$$

$$M_{51}^{tank-fl} = M_{15}^{tank-fl} \tag{30}$$

$$M_{55}^{tank-fl} = -\rho_{tank} \int_{S_t} \left(x_t^2 + z_{fl}^2\right)\, y_t\, n_y\, dS \tag{31}$$

$$M_{66}^{tank-fl} = -\rho_{tank} \int_{S_t} \left(x_t^2 + y_t^2\right)\, z_{fl}\, n_z\, dS \tag{32}$$

For heave motions, Malenica et al. indicate that no sloshing occurs in the tank. Consequently, the tank heave added mass $A_{33}^{tank-fl}$ is equal to the fluid tank mass $m^{tank-fl}$.

Static displacement of a sloshing tank causes roll and pitch moments that are reflected in the matrix $\left[C^{slosh}\right]$ in Equation (1). Within the current analysis, the sloshing tank is restricted to being symmetrical and located on the ship centreline. The sloshing tank stiffness matrix is independent of the longitudinal and vertical location onboard

ship, and has 2 non-zero terms:

$$C_{44}^{slosh} = -\rho_{tank}\, g \int_{S_t} y_t^2\, n_z\, dS \tag{33}$$

$$C_{55}^{slosh} = -\rho_{tank}\, g \int_{S_t} \left(x_t - \overline{x}_t^{fp}\right)^2\, n_z\, dS \tag{34}$$

where $\overline{x}_t^{fp}$ is the x_t coordinate of the fluid plane centroid, which is given by:

$$\overline{x}_t^{fp} = \frac{\int_{S_t} n_z\, x_t\, dS}{\int_{S_t} n_z\, dS} \tag{35}$$

5 Evaluation of Dynamic Tank Sloshing Forces to be Included in Frequency Domain Ship Motion Computations

As mentioned previously, the sloshing force terms included in ship motion computations do not consider the mass of the tank fluid in a static condition, which is already included in the ship inertial properties. Instead, the sloshing force terms consider the incremental influence of sloshing relative to the fluid being a fixed mass within the ship.

The non-zero terms of the sloshing added mass matrix are:

$$A_{11}^{slosh} = A_{11}^{tank-fl} - m^{tank} \quad (36)$$
$$A_{15}^{slosh} = A_{15}^{tank-fl} - M_{15}^{tank-fl} + z^{tank-fl}\, A_{11}^{slosh} \quad (37)$$
$$A_{22}^{slosh} = A_{22}^{tank-fl} - m^{tank} \quad (38)$$
$$A_{24}^{slosh} = A_{24}^{tank-fl} - M_{24}^{tank-fl} - z^{tank-fl}\, A_{22}^{slosh} \quad (39)$$
$$A_{26}^{slosh} = A_{26}^{tank-fl} - M_{26}^{tank-fl} + x^{tank}\, A_{22}^{slosh} \quad (40)$$
$$A_{42}^{slosh} = A_{42}^{tank-fl} - M_{42}^{tank-fl} - z^{tank-fl}\, A_{22}^{slosh} \quad (41)$$
$$A_{44}^{slosh} = A_{44}^{tank-fl} - M_{44}^{tank-fl} - z^{tank-fl}\, A_{42}^{slosh} \quad (42)$$
$$A_{46}^{slosh} = A_{46}^{tank-fl} - M_{46}^{tank-fl} + x^{tank}\, A_{42}^{slosh} \quad (43)$$
$$A_{51}^{slosh} = A_{51}^{tank-fl} - M_{51}^{tank-fl} + z^{tank-fl}\, A_{11}^{slosh} \quad (44)$$
$$A_{55}^{slosh} = A_{55}^{tank-fl} - M_{55}^{tank-fl} + z^{tank-fl}\, A_{51}^{slosh} \quad (45)$$
$$A_{62}^{slosh} = A_{62}^{tank-fl} - M_{62}^{tank-fl} + x_{tank}\, A_{22}^{slosh} \quad (46)$$
$$A_{64}^{slosh} = A_{64}^{tank-fl} - M_{64}^{tank-fl} - z^{tank-fl}\, A_{62}^{slosh} \quad (47)$$
$$A_{66}^{slosh} = A_{66}^{tank-fl} - M_{66}^{tank-fl} + x^{tank}\, A_{62}^{slosh} \quad (48)$$

where x^{tank} is the longitudinal location of the tank relative to the ship centre of gravity and $z^{tank-fl}$ is the vertical location of the tank fluid line relative to the ship centre of gravity. The sloshing damping terms are evaluated in a similar manner, but are somewhat simpler because the fluid induces zero damping force on the ship when there is no sloshing. The non-zero damping terms are as follows:

$$B_{11}^{slosh} = B_{11}^{tank-fl} \quad (49)$$
$$B_{15}^{slosh} = B_{15}^{tank-fl} + z^{tank-fl}\, B_{11}^{slosh} \quad (50)$$
$$B_{22}^{slosh} = B_{22}^{tank-fl} \quad (51)$$
$$B_{24}^{slosh} = B_{24}^{tank-fl} - z^{tank-fl}\, B_{22}^{slosh} \quad (52)$$
$$B_{26}^{slosh} = B_{26}^{tank-fl} + x^{tank}\, A_{22}^{slosh} \quad (53)$$
$$B_{42}^{slosh} = B_{42}^{tank-fl} - z^{tank-fl}\, B_{22}^{slosh} \quad (54)$$

$$B_{44}^{slosh} = B_{44}^{tank-fl} - z^{tank-fl}\, B_{42}^{slosh} \quad (55)$$
$$B_{46}^{slosh} = B_{46}^{tank-fl} + x^{tank}\, B_{42}^{slosh} \quad (56)$$
$$B_{51}^{slosh} = B_{51}^{tank-fl} + z^{tank-fl}\, B_{11}^{slosh} \quad (57)$$
$$B_{55}^{slosh} = B_{55}^{tank-fl} + z^{tank-fl}\, B_{51}^{slosh} \quad (58)$$
$$B_{62}^{slosh} = B_{62}^{tank-fl} + x_{tank}\, B_{22}^{slosh} \quad (59)$$
$$B_{64}^{slosh} = B_{64}^{tank-fl} - z^{tank-fl}\, B_{62}^{slosh} \quad (60)$$
$$B_{66}^{slosh} = B_{66}^{tank-fl} + x^{tank}\, B_{62}^{slosh} \quad (61)$$

The influence of the tank fluid on ship motion stiffness is given in Equations (33) and (34).

6 Evaluation of Dynamic Tank Sloshing Forces to be Included in Time Domain Ship Motion Computations

A new method has been developed for evaluating tank sloshing forces to be used with time domain ship motion computations. The approach is similar to that used for computing ship hydrodynamic forces in the time domain in Reference 8. The equations of motion in the time domain are expressed as:

$$\begin{aligned}\Big([M] \;+\; [A(\omega_e=\infty)] \;+\; [A^{slosh}(\omega_e=\infty)]\Big)\;\{\ddot{\eta}(t)\} \\ +\,[b(U)]\;\{\dot{\eta}(t)\} \;+\; \int_0^{\tau_{max}} [K(\tau)]\;\{\dot{\eta}(t-\tau\}\;d\tau \\ +\int_0^{\tau_{max}} [K^{slosh}(\tau)]\;\{\dot{\eta}(t-\tau\}\;d\tau \\ +\;\Big([C] \;+\; [c(U)] \;+\; [C^{slosh}]\Big)\;\{\eta(t)\} \;=\; \{F_I(t)\} \;+\; \{F_D(t)\} \qquad (62)\end{aligned}$$

where $[b(U)]$ is the speed dependent hull damping matrix, $[K(\tau)]$ is the hull retardation function matrix for delay time τ, τ_{max} is the maximum considered delay time, $[K^{slosh}(\tau)]$ is the sloshing retardation function matrix for delay time τ, and $[c(U)]$ is the speed dependent hull stiffness matrix. The presence of retardation functions in Equation (62) is due to forces acting on the ship being dependent on the previous motions of the ship. The retardation functions decay to zero for large τ, and the integration limit τ_{max} should be selected accordingly.

The sloshing retardation functions can be computed using either of the following two equations adapted from computations for ship hulls in Reference 8:

$$K_{jk}^{slosh}(\tau) \;=\; -\frac{2}{\pi}\int_0^{\infty}\Big(A_{jk}^{slosh}(\omega_e) \;-\; A_{jk}^{slosh}(\infty)\Big)\;\omega_e\;\sin(\omega_e\,\tau)\;d\omega_e \qquad (63)$$

$$K_{jk}^{slosh}(\tau) \;=\; \frac{2}{\pi}\int_0^{\infty} B_{jk}^{slosh}(\omega_e)\cos(\omega_e\,\tau)\;d\omega_e \qquad (64)$$

When evaluating the above integrals for tank sloshing, care must be taken due to the great variation of added mass and damping coefficients with encounter frequency, as demonstrated in Figures 5 and 6.

When evaluating and using the sloshing retardation functions, a primary requirement is to be able to model the dependence of sloshing phenomena on frequency of motion. Fortunately, the added mass can be re-evaluated using the retardation functions, which offers a method for verifying the fidelity of the computed retardation functions:

$$A_{jk}^{slosh}(\omega_e) \;=\; A_{jk}^{slosh}(\infty) \;-\; \frac{1}{\omega_e}\int_0^{\infty} K_{jk}^{slosh}(\tau)\;\sin(\omega_e\,\tau)\;d\tau \qquad (65)$$

Correct modelling of the low frequency behaviour in the time domain requires that the retardation functions satisfy the following based on Equation (65) at the limit of $\omega_e \to 0$:

$$A_{jk}^{slosh}(0) \; - A_{jk}^{slosh}(\infty) \;\; = \;\; - \frac{1}{\omega_e} \int_0^\infty K_{jk}^{slosh}(\tau) \; \tau \; d\omega_e \tag{66}$$

The above equation indicates that correct modelling of low frequency behaviour is very dependent on the retardation functions at large values of delay time τ. In practice, a finite limit τ_{max} must be set for evaluation of non-zero retardation functions. Initial computation indicated poor modelling of time domain hydrodynamic forces at very low frequencies when using retardation functions evaluated to finite values of τ_{max}. Fortunately, it has been found that the following modified retardation functions can be used to give very good time domain results across the entire frequency range:

$$K_{jk}^{slosh}(\tau) \;\; = \;\; \left(1 \; - \; \frac{\tau}{\tau_{max}}\right) \frac{2}{\pi} \int_0^\infty B_{jk}^{slosh}(\omega_e) \cos(\omega_e \, \tau) \; d\tau \tag{67}$$

Note that τ_{max} must be large enough to capture the behaviour of the retardation function.

When evaluating retardation functions using Equations (64) and (67), damping coefficients within the integrals are only available to a finite maximum encounter frequency, denoted here as ω_e^*. To account for damping at frequencies beyond the range of computation, an approach similar similar to that presented by Nam et al. [10] is used, with damping at high encounter frequencies being approximated by:

$$B_{jk}^{slosh}(\omega_e) \;\; = \;\; B_{jk}^{slosh}(\omega_e^*) \left(\frac{\omega_e^*}{\omega_e}\right)^2 \text{ for } \omega_e > \omega_e^* \tag{68}$$

Equation (64) can then be evaluated as follows:

$$\begin{aligned} K_{jk}^{slosh}(\tau) \;\; = \;\; & \frac{2}{\pi} \int_0^{\omega_e^*} B_{jk}^{slosh}(\omega_e) \cos(\omega_e \, \tau) \; d\omega_e \\ & + \frac{2}{\pi} \; B_{jk}^{slosh}(\omega_e^*) \; \omega_e^* \left[\cos\left(\omega_e^* \; \tau\right) \; + \; \omega_e^* \; \tau \; \mathrm{si}(\omega_e^*)\right] \end{aligned} \tag{69}$$

where $\mathrm{si}(x)$ is the sine integral function defined by:

$$\mathrm{si}(x) \;\; = \;\; - \int_x^\infty \frac{\sin t}{t} \; dt \tag{70}$$

Similarly, Equation (67) including the time-dependent correction to the retardation function can be evaluated by:

$$\begin{aligned} K_{jk}^{slosh}(\tau) \;\; = \;\; & \left(1 \; - \; \frac{\tau}{\tau_{max}}\right) \left(\frac{2}{\pi} \int_0^{\omega_e^*} B_{jk}^{slosh}(\omega_e) \cos(\omega_e \, \tau) \; d\omega_e \right. \\ & \left. + \frac{2}{\pi} \; B_{jk}^{slosh}(\omega_e^*) \; \omega_e^* \left[\cos\left(\omega_e^* \; \tau\right) \; + \; \omega_e^* \; \tau \; \mathrm{si}(\omega_e^*)\right]\right) \end{aligned} \tag{71}$$

Example time domain computations have been performed for the 4 m by 4 m by 2 m tank introduced in Section 4. For the present computations, the tank fluid line is located at the ship centre of gravity. Figure 9 shows the sway retardation functions computed with and without a correction for the maximum time delay τ_{max} applied (i.e. using Equations (71) and (69) respectively). The retardation functions were computed using an encounter frequency increment of 0.05 rad/s. Figure 9 shows the decay of the retardation functions with time, and suggests that the oscillation of the uncorrected function at large τ might be due to numerical approximations rather that actual physical behaviour.

Figure 10 shows sway added mass computed directly in the frequency domain and computed indirectly using Equation (65) based on the retardation with the correction the maximum time delay τ_{max} applied. The added mass computed from the retardation function gives excellent agreement with the directly computed added mass at the low and high frequency limits. There is some difference between the two forms at intermediate frequencies; however, the difference is minor relative to uncertainties related to fluid damping.

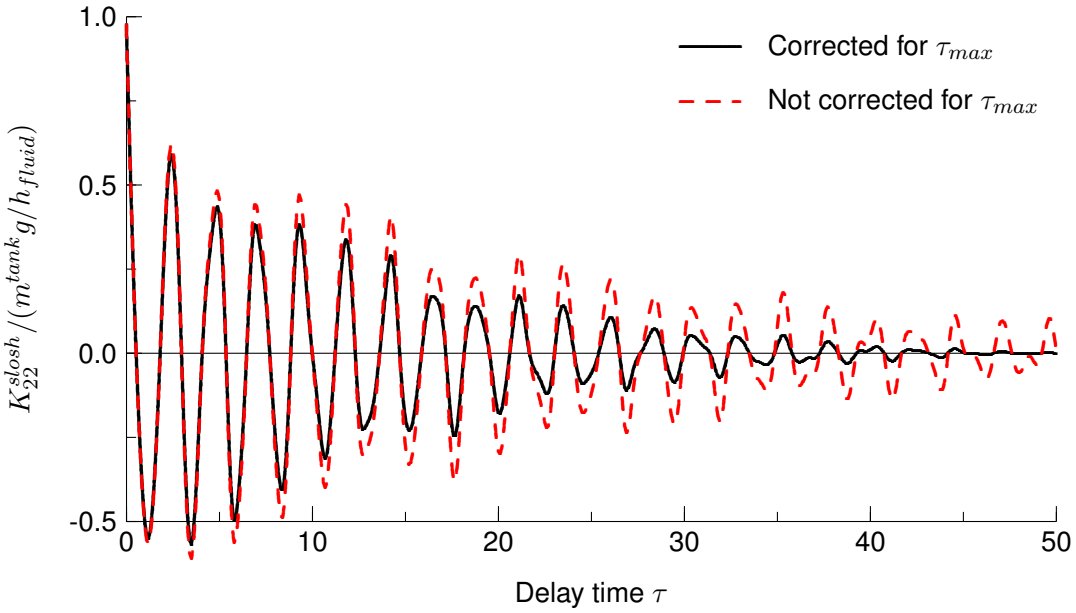

Figure 9: *Sway Sloshing Retardation Function for 4 m by 4 m by 2 m Tank, Peak Fluid Damping Coefficient* $\hat{\epsilon}_{tank} = 0.05$

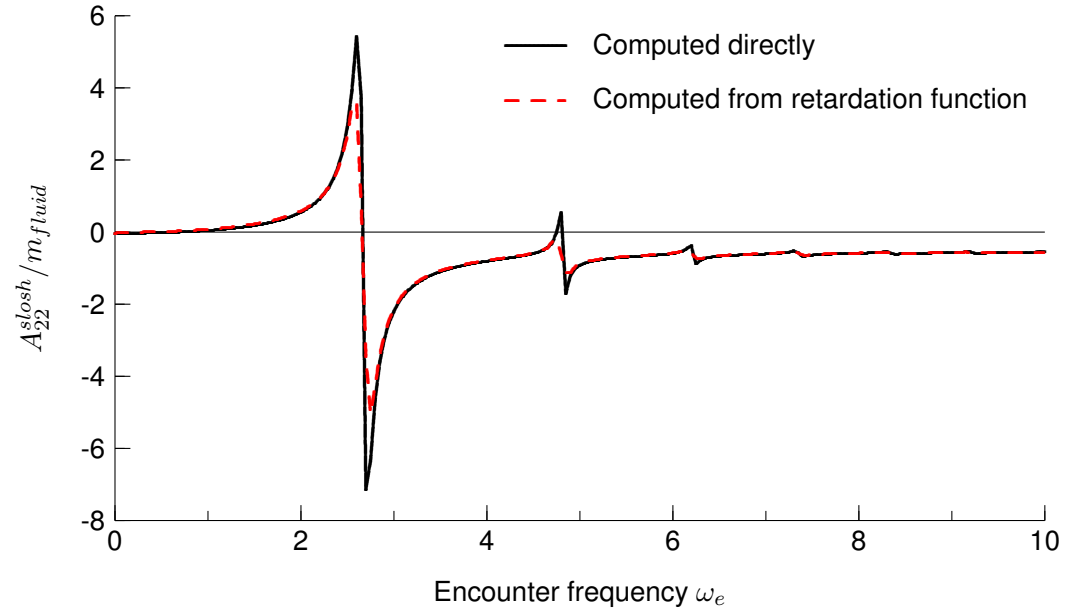

Figure 10: *Sway Sloshing Added Mass from Direct Frequency Domain Computation and from Retardation Function for 4 m by 4 m by 2 m Tank, Peak Fluid Damping Coefficient* $\hat{\epsilon}_{tank} = 0.05$

7 Parametric Studies of Sloshing Computations

Parametric studies have been performed to ensure that the implemented sloshing method is providing consistent results. The parametric studies also demonstrate convergence of results with refinements to the geometric mesh and number of encounter frequencies used for computation.

7.1 Sloshing Coefficients for a 1 m by 1 m by 0.5 m Tank

Sloshing coefficients have been computed for a 1 m by 1 m by 0.5 m tank, with dimensions half of those used for the tank computations in Section 4. The peak fluid damping factor for the smaller tank $\hat{\epsilon}_{tank}$ has a value of 0.05, the same as the value for the larger tank. Applying Froude scaling when modelling the smaller tank, the lower frequency for maximum damping $\omega^{\hat{\epsilon}}_{lower}$ has been set to 4 rad/s and the upper frequency for maximum damping $\omega^{\hat{\epsilon}}_{lower}$ has been set to 16 rad/s.

Figure 11 shows added mass and damping coefficients for the 1 m by 1 m by 0.5 m tank. Taking into account that frequencies for the smaller tank are twice as large as those for the larger tank due to Froude scaling, the computed results for the smaller tank shown in Figure 11 are identical to the results for the larger tank shown in Figures 5 and 6.

7.2 Sloshing Coefficients for a 4 m by 4 m by 0.5 m Tank

To examine the influence of water depth on sloshing behaviour, sloshing coefficients have been computed for the tank with horizonal dimensions of 4 m by 4 m tank used in Section 4 but with the water height reduced from 2 m to 0.5 m. Sway and roll sloshing coefficients for the tank with 0.5 m fluid height are shown in Figures 12 and 13, and can be compared with coefficients for the tank with 2 m fluid height shown in Figure 5 to Figure 8. For both fluid heights, the sway added mass at low frequency is equal to the mass of the fluid. This behaviour occurs for both surge and sway because the fluid simply translates with the motions of the tank at low frequency. The roll added mass coefficient increases significantly as the fluid depth decreases. This behaviour likely occurs because the fluid depth is small relative to the width of the tank, causing the fluid flow to be highly dependent on water depth as discussed by Newman [5]. It should be noted that nonlinear geometric effects will be significant when fluid depth is small relative to tank width.

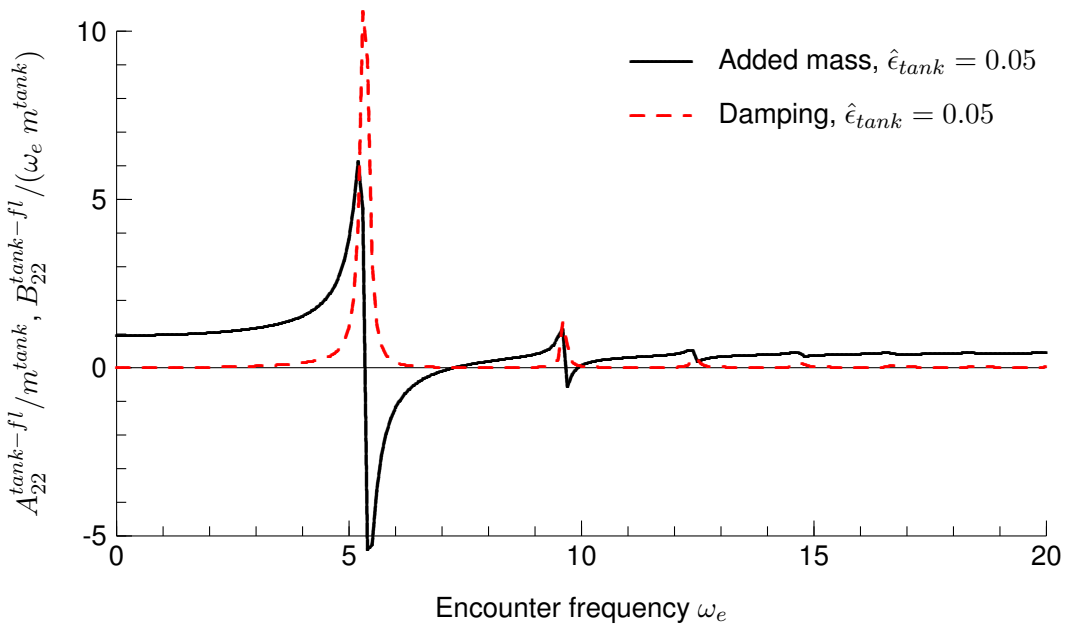

Figure 11: *Sway Added Mass and Damping for 1 m by 1 m by 0.5 m Tank, Peak Fluid Damping Coefficient* $\hat{\epsilon}_{tank} = 0.05$

7.3 Dependency of Sloshing Coefficients on Mesh for a 4 m by 4 m by 2 m Tank

Computations have been performed to examine the dependency of sloshing coefficients on mesh size for a 4 m by 4 m by 2 m tank. Figures 14 and 15 show results using the base mesh used for previous computations and using meshes that are coarser and finer. The computed coefficients show only small variation with the number of panels, indicating satisfactory convergence of results with mesh size.

7.4 Dependency of Sloshing Coefficients on Encounter Frequency Increment for a 4 m by 4 m by 2 m Tank

Computations in the frequency domain and sloshing retardation functions are dependent on the encounter frequency increment. The encounter frequency increment must be sufficiently small to capture the variation of sloshing coefficients with encounter frequency. Figures 16 and 17 show sway added mass and damping coefficients for different encounter frequency increments. Figure 18 shows sway retardation functions computed using the different encounter frequency increments. The computed results show good convergence of results for the two smaller encounter frequency increments.

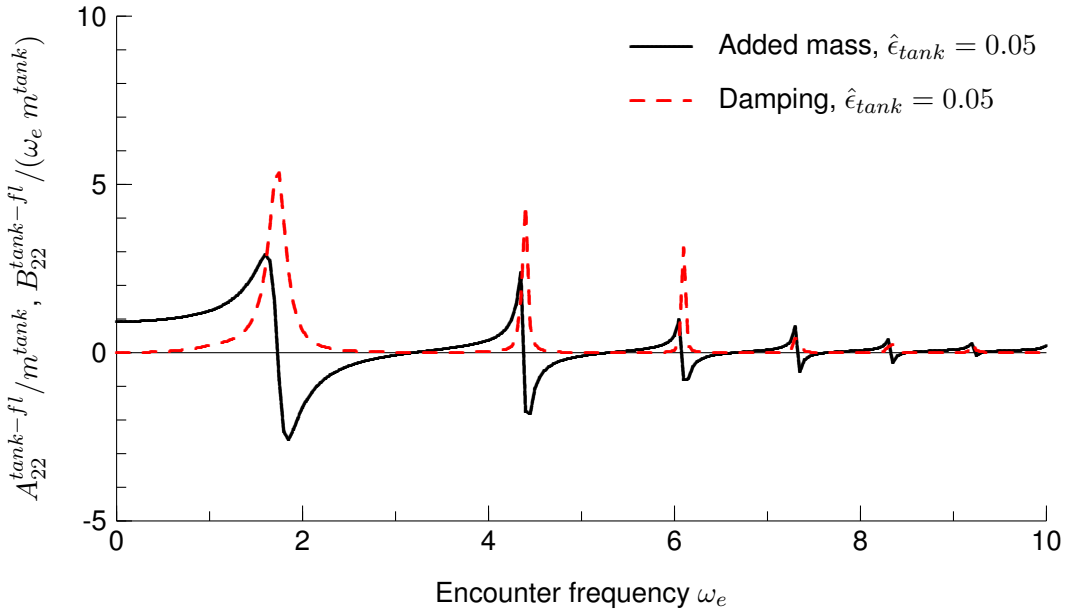

Figure 12: *Sway Added Mass and Damping for 4 m by 4 m by 0.5 m Tank, Peak Fluid Damping Coefficient* $\hat{\epsilon}_{tank} = 0.05$

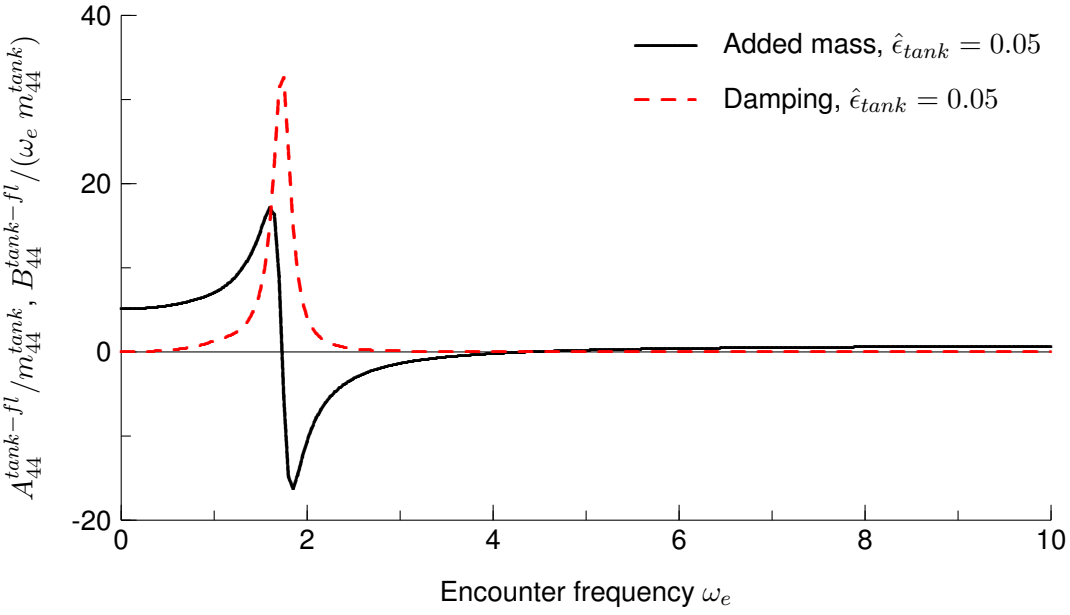

Figure 13: *Roll Added Mass and Damping for 4 m by 4 m by 0.5 m Tank, Peak Fluid Damping Coefficient* $\hat{\epsilon}_{tank} = 0.05$

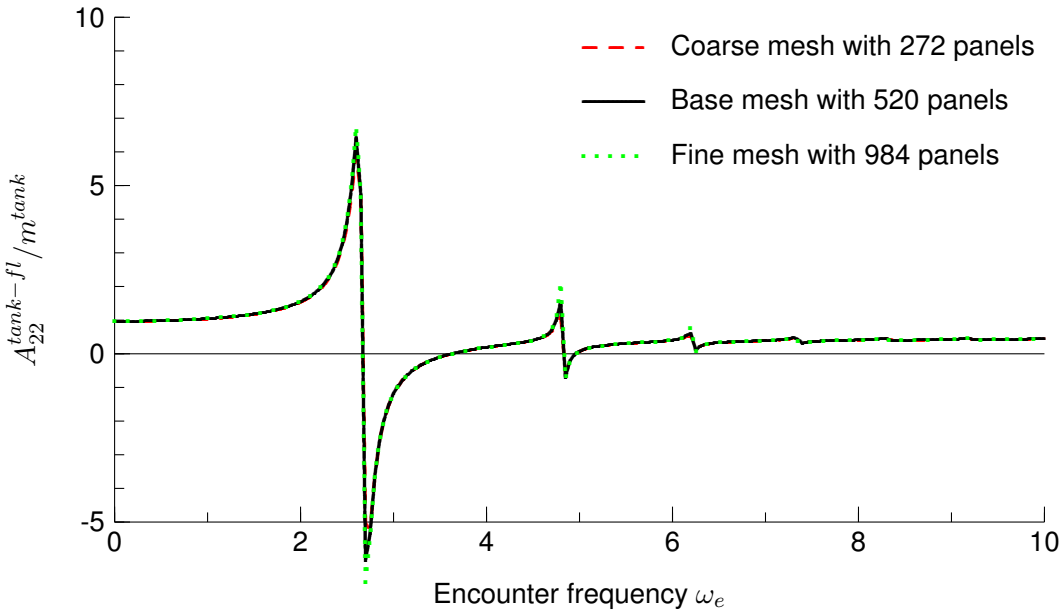

Figure 14: *Sway Added Mass for 4 m by 4 m by 2 m Tank with Different Geometry Meshes*

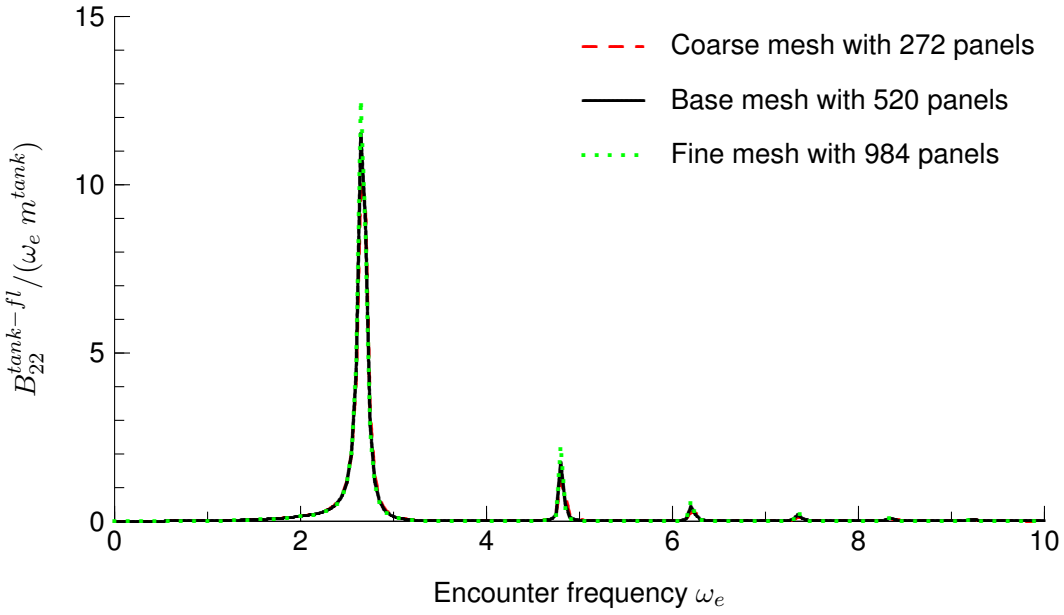

Figure 15: *Sway Damping for 4 m by 4 m by 2 m Tank with Different Geometry Meshes*

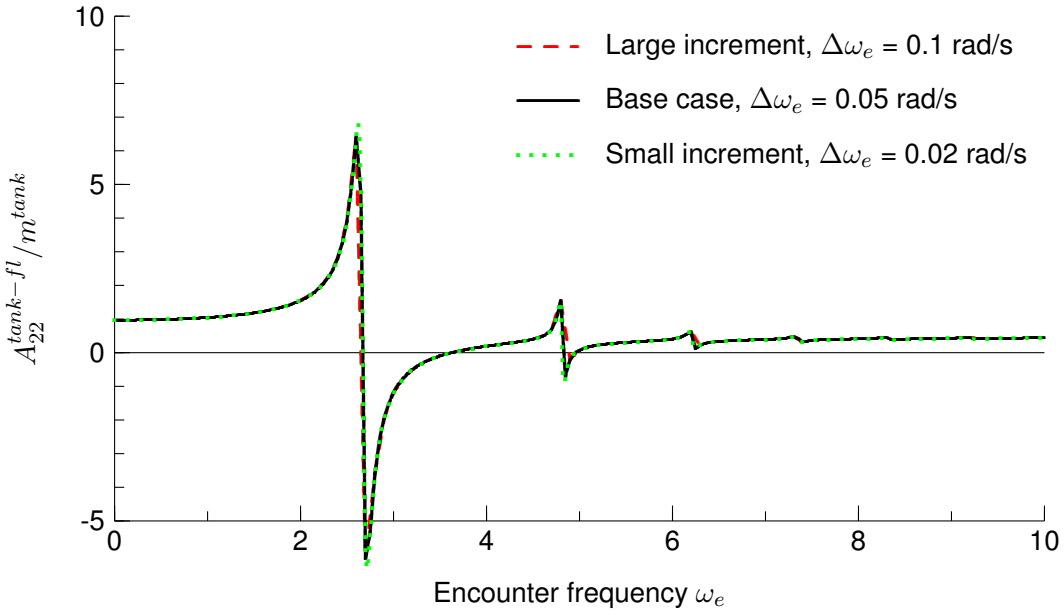

Figure 16: *Sway Added Mass for 4 m by 4 m by 2 m Tank with Different Encounter Frequency Increments*

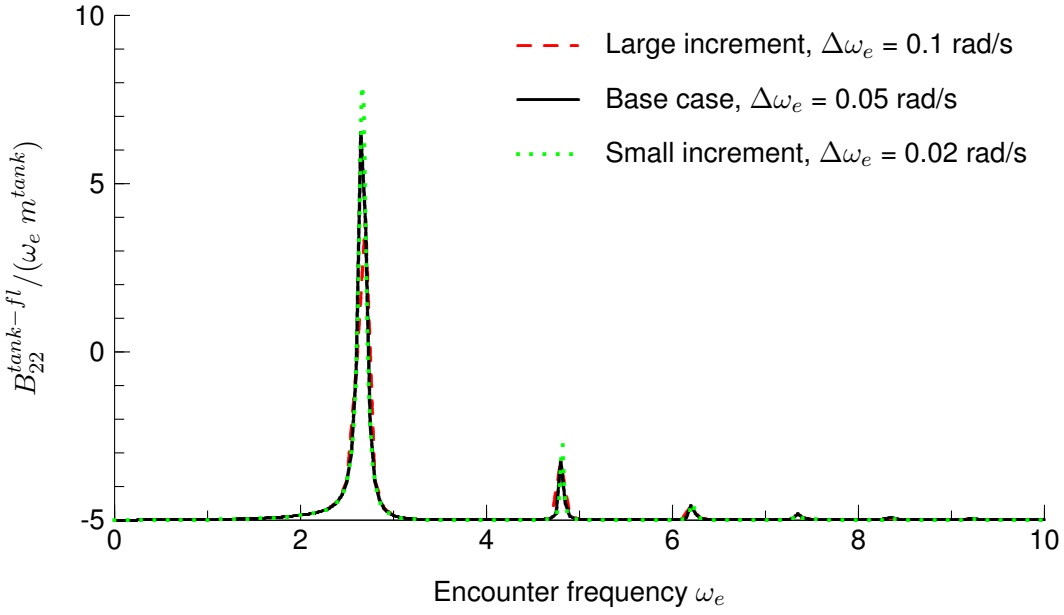

Figure 17: *Sway Damping for 4 m by 4 m by 2 m Tank with Different Encounter Frequency Increments*

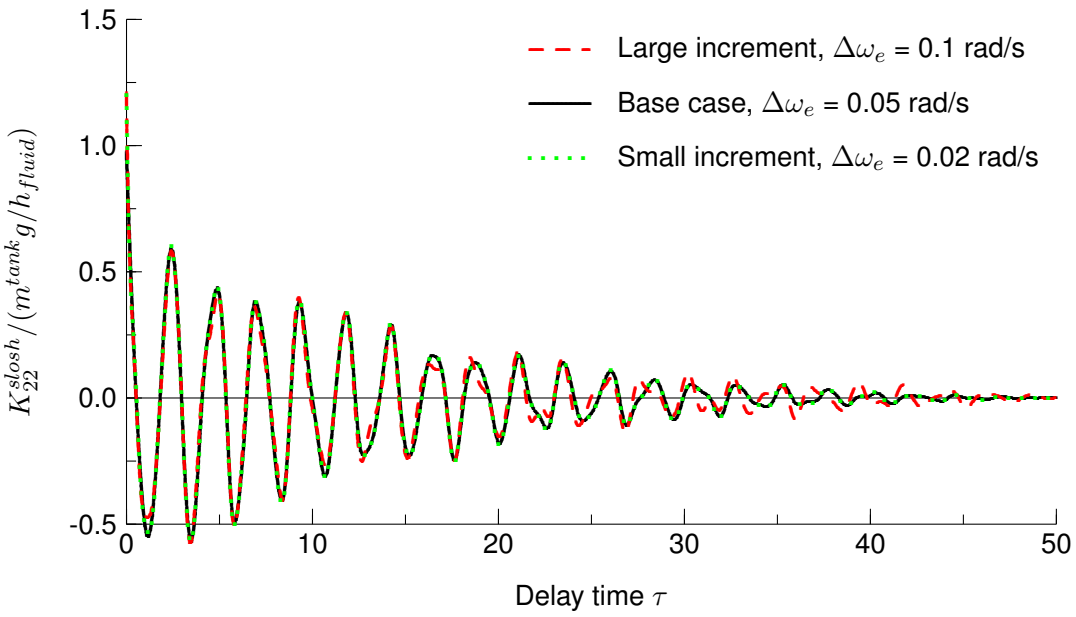

Figure 18: *Sway Retardation Functions for 4 m by 4 m by 2 m Tank with Different Encounter Frequency Increments*

8 Validation of Roll Motions for a Barge Model with Two Sloshing Tanks

Roll motion predictions have been validated using experimental data for a barge model tested by Molin et al. [9]. Table 2 gives the dimensions of the barge. Two sloshing tanks were placed on the deck of the barge, and Figure 3 gives the dimensions for each tank. The tank dimensions in Table 3 are given using the ShipMo3D conventions for length and width, with tank length being along the ship longitudinal axis axis and tank width being along the ship lateral axis (Molin et al. use the opposite convention for tank length and width). Table 4 gives the inertial properties of the barge, which are required as inputs to ShipMo3D.

Table 2: *Barge Dimensions*

Length, L	3.0 m
Beam, B	1.0 m
Total depth	0.267 m
Draft, T	0.108 m

Table 3: *Barge Sloshing Tank Dimensions*

Length, L_{tank}	0.25 m
Width, w_{tank}	0.80 m
Total height, h_{tank}	0.267 m
Fluid height, h_{fluid}	0.19 m
Height above baseline, z_{bl}^{tank}	0.30 m

Roll motion predictions are sensitive to the modelling of viscous forces. Molin et al. indicate that the following roll damping equation can be used to model the observed experimental behaviour of the barge:

$$F_4^{hull-eddy} = -\frac{1}{2}\,\rho\,C_d\,B^4\,L\,|\dot{\eta}_4|\,\dot{\eta}_4 \tag{72}$$

where $F_4^{hull-eddy}$ is the hull eddy damping force, C_d is the drag coefficient, and $\dot{\eta}_4$ is the ship roll velocity. ShipMo3D uses a similar approach but with different dimensional

Table 4: *Inertial Properties of Barge with Two Sloshing Tanks with Fluid Height of 0.19 m*

	Mass	KG	r_{xx} (wrt own KG)
Barge	169 kg	0.240 m	0.414 m
Tanks	76 kg	0.395 m	0.237 m
Ballast masses	40 kg	0.280 m	0.35 m
Total	285 kg	0.287 m	0.372 m

terms as follows (see Reference 11):

$$F_4^{hull-eddy} \;=\; -\frac{1}{4}\,\rho\,C_{eddy}^{hull}\int_{S_{hull}} n_4^2\,\sqrt{y^2\;+\;z^2}\,dS\;\;|\dot{\eta}_4|\;\;\dot{\eta}_4 \tag{73}$$

Molin et al. assign the drag coefficient C_d a value of 0.2 based on experimental observations. Analysis of the hull geometry gives an associated value of 8.6 for the ShipMo3D input coefficient C_{eddy}^{hull}.

Figure 19 compares predicted frequency domain and experimental roll RAOs for the barge in a seaway modelled by a JONSWAP spectrum with significant wave height H_s of 0.066 m, peak wave period T_p of 1.6 s, and peak enhancement factor γ of 2.0. The experiments were conducted in finite water depth of 3 m, while the ShipMo3D predictions are in water of infinite depth; thus, the data comparison is given for encounter frequencies of 3 rad/s and greater, for which the assumption of deep water is applicable (water depth/wavelength > 0.5). The numerical predictions compare favourably with the experimental data. The water in the sloshing tanks is 27 percent of the total mass and is located high relative to the total centre of gravity; thus, sloshing likely has a large influence on the total roll motion.

Additional ShipMo3D predictions were made in regular waves of steepness $H/\lambda = 0.0165$, which is based on the significant wave height of 0.066 m and the peak wave period of 1.6 s for the random wave experiments. Figure 20 shows that the ShipMo3D time domain predictions give very good agreement with the frequency domain predictions, suggesting correct implementation in the time domain.

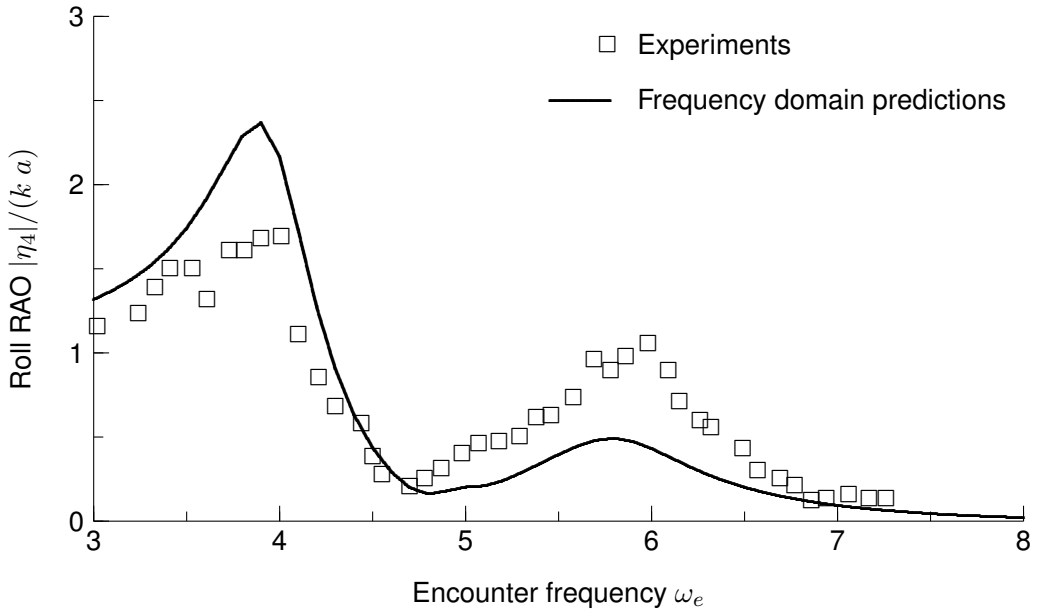

Figure 19: *Barge Model Roll RAOs in Beam Seas with JONSWAP Spectrum, $H_s = 0.066$ m, $T_p = 1.6$ s, $\gamma = 2.0$*

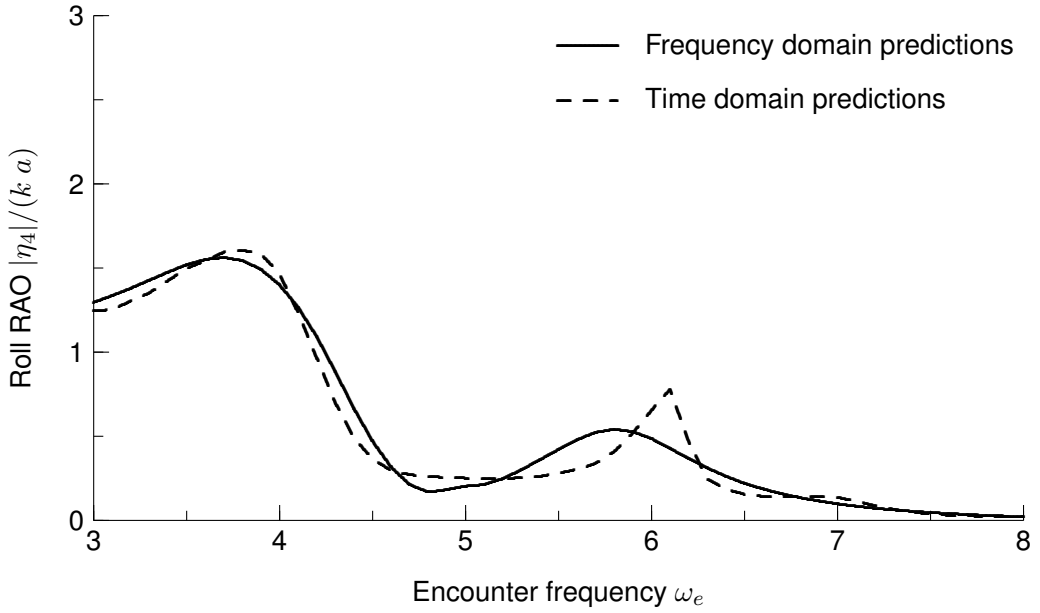

Figure 20: *Barge Model Roll RAOs in Regular Beam Seas, Wave Steepness $H/\lambda = 0.0165$*

9 Example Case of Sloshing Tank for Roll Stabilization of a Generic Frigate

This section presents an example design of a sloshing tank for roll stabilization of a generic frigate. Table 5 gives the properties of the generic frigate, which was used for a similar example for a U-tube tank in Reference 3.

Table 5: *Generic Frigate Properties*

Length between perpendiculars, L_{pp}	120.0 m
Draft at midships, T_{mid}	4.2 m
Trim by stern, t_{stern}	0.0 m
Displacement, $\triangle$	3713 tonnes
Height of CG above baseline, $\overline{KG}$	6.0 m
Metacentric height, $\overline{GM}$	1.43 m
Natural roll frequency, ω_4	0.704 rad/s
Breadth at midships	15.0 m
Hull depth at midships	9.4 m

9.1 Preliminary Design of a Box-Shaped Tank

A box-shaped tank was initially designed to stabilize the roll motions of the generic frigate. To obtain roll stabilization, it was important for the tank to have a sway natural frequency near the roll frequency of the frigate. Based on the ship geometry, the maximum width of the tank was specified as 12 m. Figure 21 shows sloshing frequency versus fluid height for box-shaped tanks with widths of 8 m, 10 m, and 12 m. To match the ship natural roll frequency, a tank with width of 12 m and fluid height of 0.7 m was selected. The decision to select the maximum tank width was based on the benefit of maximizing the ratio of fluid height to tank width to minimize saturation of the box-shaped tank (saturation occurs when the water piles up at one side of the tank).

The box-shaped tank is filled with fresh water ($\rho_{tank} = 1000$ kg/m^3) for ease of operation and maintenance. Guidelines for design of U-tube tanks presented in Reference 3 are useful for design of the flume tank. To maintain static stability, the allowable

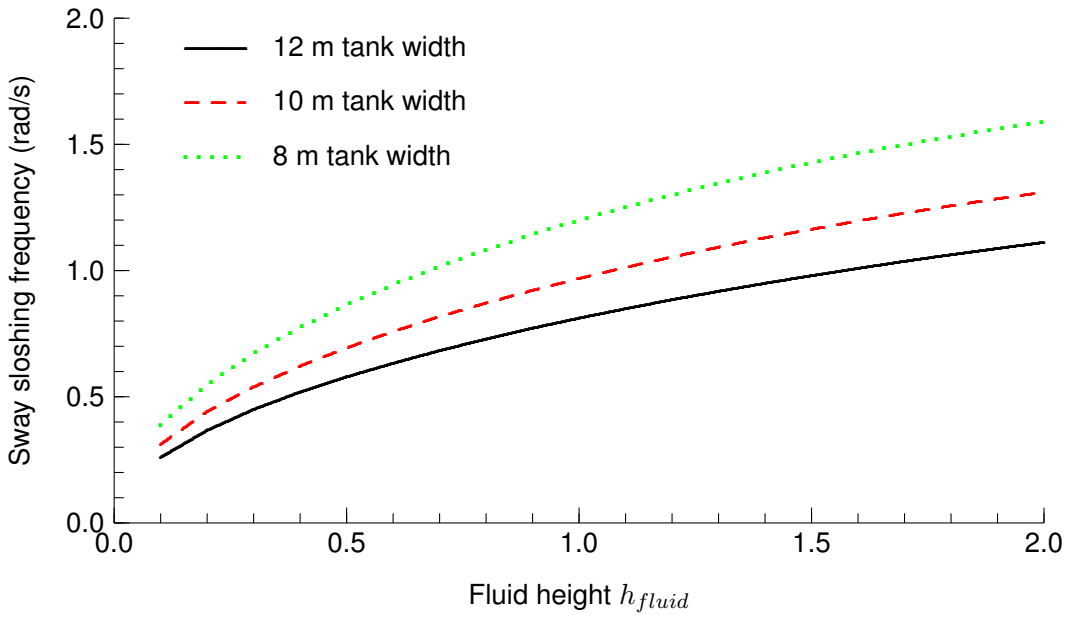

Figure 21: *Sway Sloshing Natural Frequency for Box Sloshing Tank*

effective reduction in metacentric height is limited to 0.2 m. For the box-shaped flume tank, the effective change to the ship metacentric height is given by:

$$\Delta\overline{GM} = -\frac{\rho_{tank}\ L_{tank}\ w_{tank}^3}{12\ \triangle} \tag{74}$$

where L_{tank} is the length of the tank along the ship longitudinal axis, w_{tank} is the width of the tank, and $\triangle$ is the ship mass displacement. A tank length of 5.0 m was selected to keep the reduction in metacentric height less than 0.2 m. The resulting tank fluid mass is 1.3 percent of the ship mass, which is consistent with U-tube tank installations that are typically between 1 and 5 percent of ship mass.

9.2 Finalized Design of a Flume Tank with Narrow Middle

The preliminary box-shaped tank was modified to obtain a flume tank with a narrow middle portion as shown in Figure 22. The flume tank with a narrow middle has the benefit of a higher fluid height for a given sway sloshing frequency, reducing the occurrence of saturation as roll motions increase. The designed flume tank has a fluid height of 1.2 m, significantly greater than the fluid height of 0.7 m for the box-shaped tank.

The flume tank was modelled with 892 panels on the wetted surface and a peak fluid

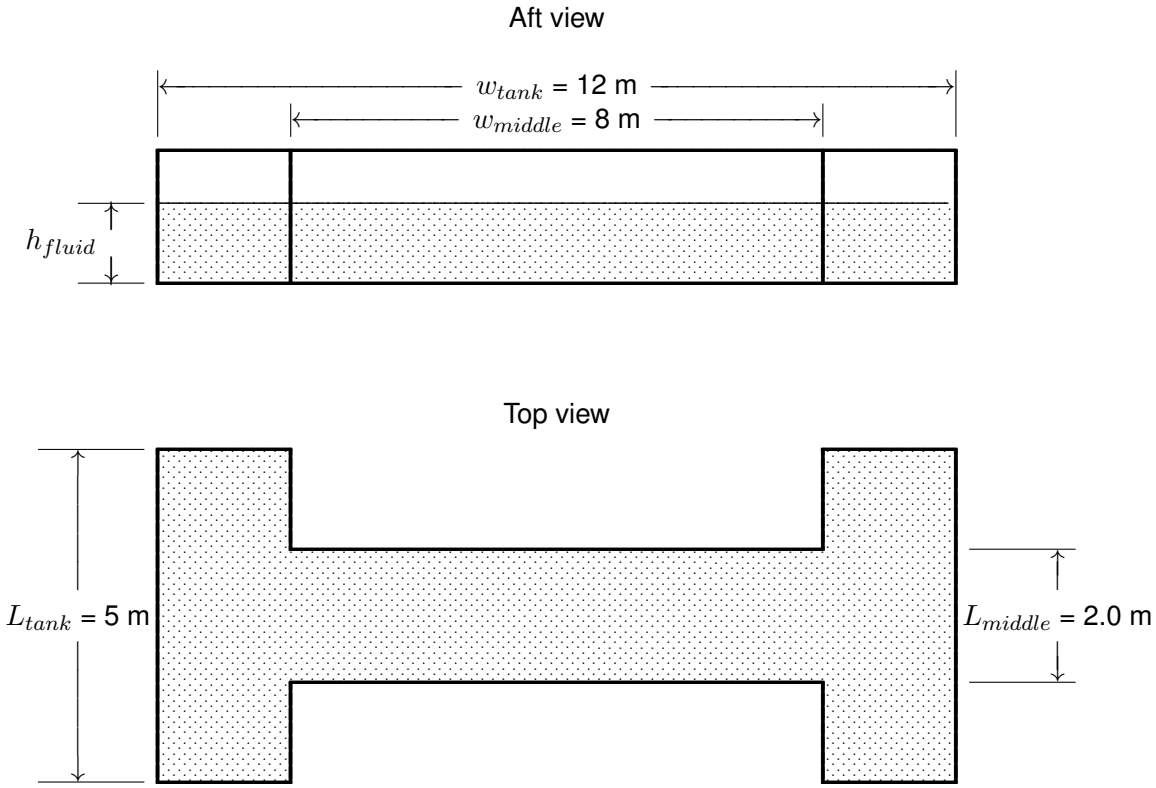

Figure 22: *Flume Tank with Narrow Middle for Generic Frigate*

damping factor of 0.02 applied to encounter frequencies from 0.3 rad/s to 8.0 rad/s. Figures 23 and 24 show added mass and damping coefficients for sway and roll. Figure 23 shows that the selected frequency range captures several sway sloshing modes. The most surprisingly result is the large magnitude of roll added mass and damping coefficients for the tank. Due to the small ratio of fluid height to tank width, the roll forces acting on the tank are primarily influenced by the vertical motion within the tank. As discussed by Newman, vertical forces of large magnitude can arise within a tank, which are the likely cause of the large roll sloshing forces for the present tank.

Figures 25 and 26 show the sway and roll sloshing retardation function for the generic frigate roll tank. The maximum selected delay time of 50 s appears to capture the behaviour of the retardation functions.

Seakeeping computations have been performed for the generic frigate with no flume tank, and with the flume tank bottom located 6 m and 8 m above the ship baseline. Sea state 5 is modelled with a Bretschneider spectrum with significant wave height H_s of 3.25 m and peak wave period T_p of 9.7 s. Figure 27 shows that the presence of a flume tank reduces roll motions by approximately 25 percent. The vertical position of the flume tank has little influence on the ship roll motions because the vertical forces acting on the flume tank are dominant. For a flume tank with a higher fluid height to width ratio, horizontal forces would become more important, thus causing the vertical location of the flume tank to become more important.

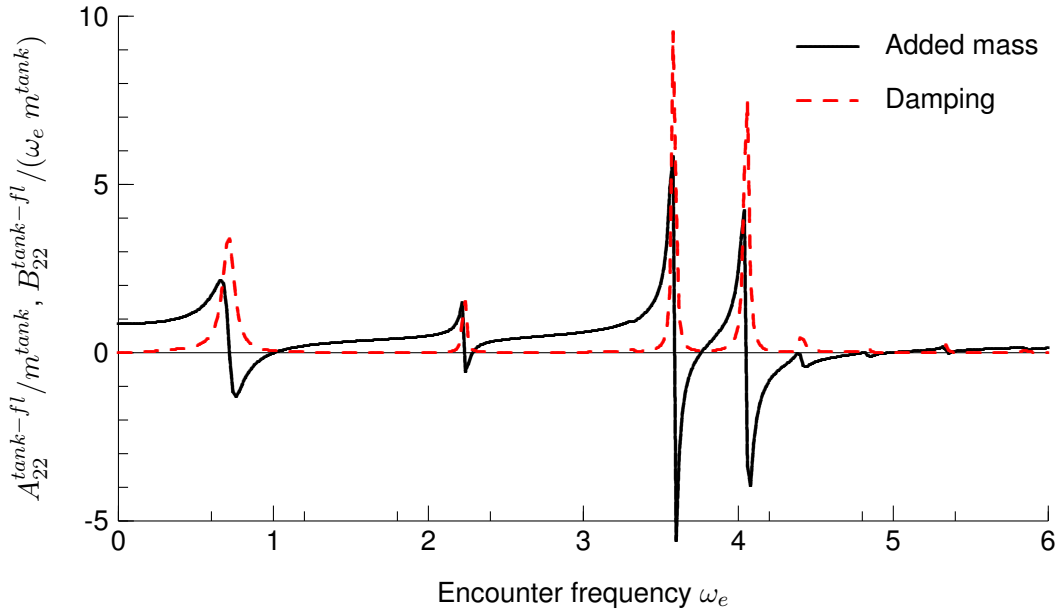

Figure 23: *Sway Sloshing Added Mass and Damping for 5 m by 12 m by 1.2 m Flume Tank with Narrow Middle for Generic Frigate*

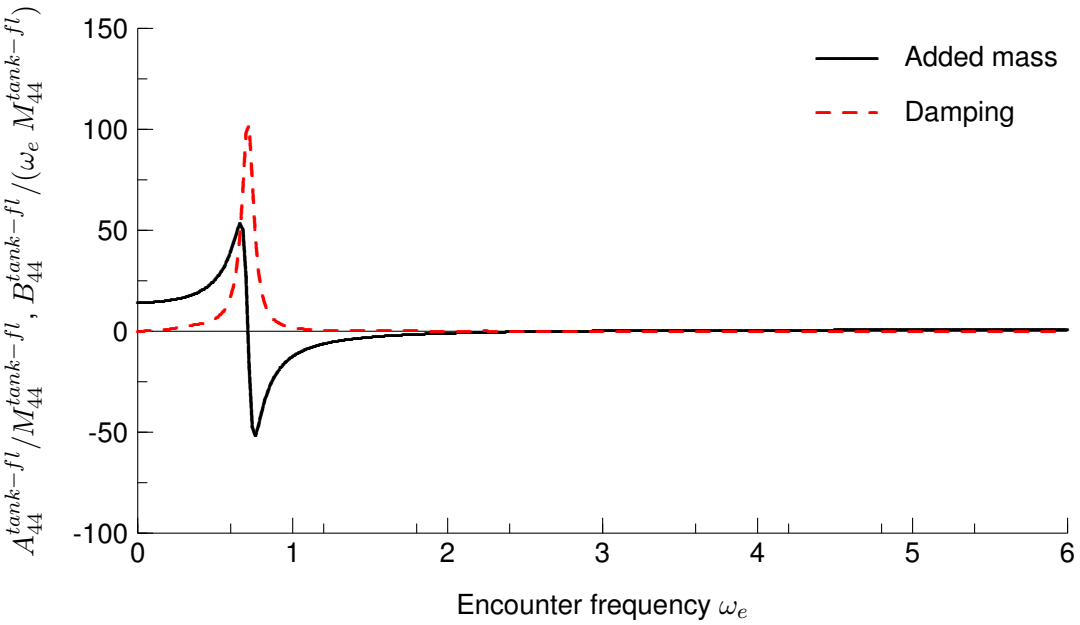

Figure 24: *Roll Sloshing Added Mass and Damping for 5 m by 12 m by 1.2 m Flume Tank with Narrow Middle for Generic Frigate*

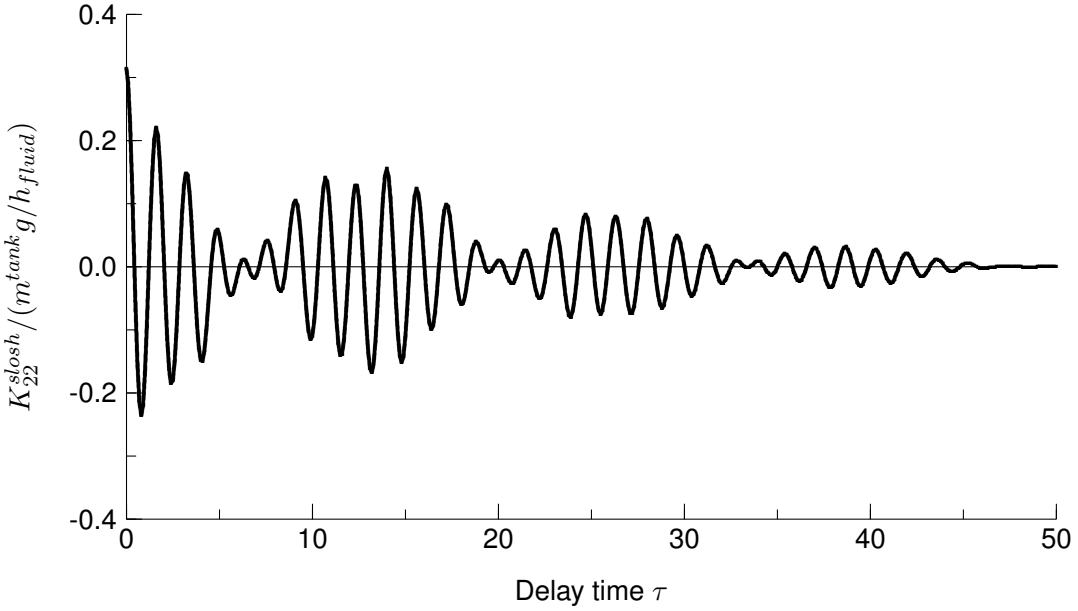

Figure 25: *Sway Sloshing Retardation Function for 5 m by 12 m by 1.2 m Flume Tank with Narrow Middle for Generic Frigate*

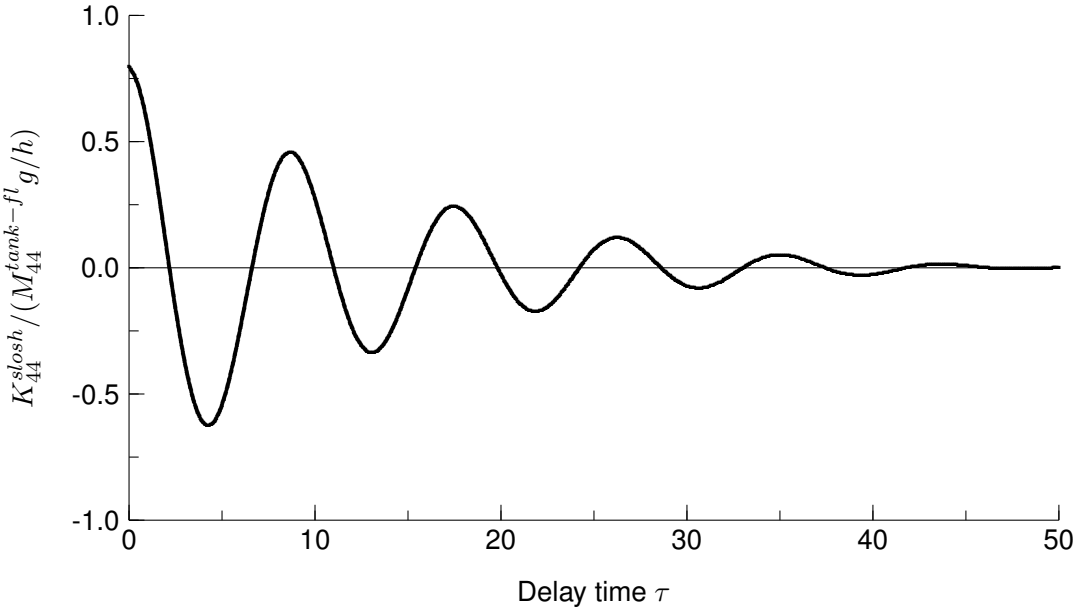

Figure 26: *Roll Sloshing Retardation Function for 5 m by 12 m by 1.2 m Flume Tank with Narrow Middle for Generic Frigate*

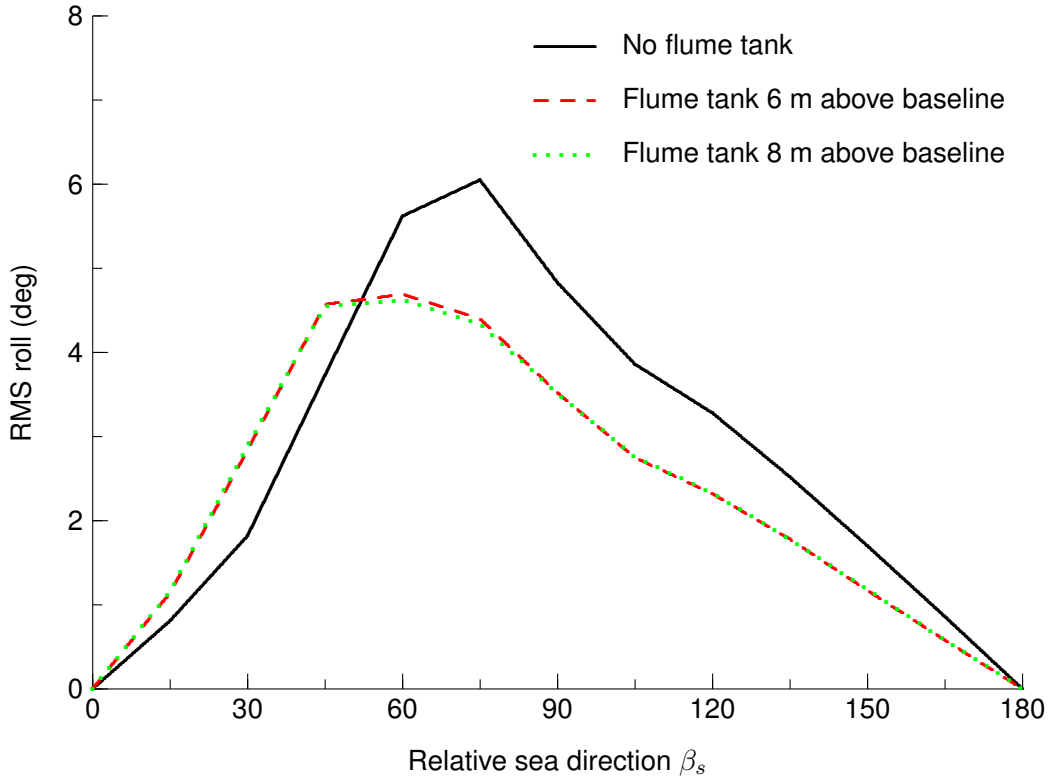

Figure 27: *RMS Roll for Generic Frigate in Sea State 5, Bretschneider Spectrum, Significant Wave Height $H_s = 3.25$ m, Peak Wave Period $T_p = 9.7$ s*

10 Discussion

The implemented method for predicting sloshing forces is robust and is giving promising results. Computed sloshing forces give excellent convergence with refinement of the geometric mesh, and sloshing force coefficients for a tank can typically be computed with less than one hour of computation time.

Computed sway (and surge) sloshing forces behave as expected. Computed sway added mass coefficients approach 1.0 at low frequencies when static fluid mass is included in the sway added mass, which is the case for the coefficient $A_{22}^{tank-fl}$. For a box-shaped tank, computed sway natural frequencies agree with analytical values.

Computed roll (and pitch) non-dimensional sloshing force coefficients demonstrate large dependence on water depth. The dependence of roll sloshing forces on water depth is likely due to the influence of the sensitivity of sloshing flow to vertical motion, as discussed by Newman [5]. Nonlinear geometric effects will also cause roll sloshing force coefficients to vary with with water depth. Further investigation regarding the variation of roll force coefficients with water depth would likely be worthwhile.

A non-dimensional peak damping coefficient $\hat{\epsilon}_{tank}$ has been introduced to account for viscous forces within the tank. The computations appear to give realistic results when the peak damping coefficient has a value in the range between 0.01 and 0.05. Future studies utilizing experiments or computational fluid dynamics would be useful for developing more specific guidelines regarding input peak damping.

11 Conclusions

A potential flow method has been implemented for modelling the influence of tank sloshing on ship motions. The method is robust and computationally efficient. Computed results for translational modes (surge and sway) behave as expected, with added mass approaching static fluid mass at low frequencies and predicted sloshing frequencies agreeing with analytical solutions. Computed roll sloshing coefficients show large dependence on water depth when water depth is small relative to tank horizontal dimensions, and it is recommended that this phenomenon be investigated further. Predicted roll motions for a barge model with sloshing tanks show good agreement with experimental values.

References

[1] McTaggart, K. (2012), ShipMo3D Version 3.0 User Manual for Creating Ship Models, (DRDC Atlantic TM 2011-307) Defence Research and Development Canada – Atlantic.

[2] McTaggart, K. (2012), ShipMo3D Version 3.0 User Manual for Computing Ship Motions in the Time and Frequency Domains, (DRDC Atlantic TM 2011-308) Defence Research and Development Canada – Atlantic.

[3] McTaggart, K. (2012), Modelling of U-tube Tanks for ShipMo3D Ship Motion Predictions, (DRDC Atlantic ECR 2011-300) Defence Research and Development Canada – Atlantic.

[4] Malenica, S., Zalar, M., and Chen, X. (2003), Dynamic Coupling of Seakeeping and Sloshing, In *Thirteeth International Offshore and Polar Engineering Conference*, Honolulu, Hawaii.

[5] Newman, J. (1989), Wave Effects on Vessels with Internal Tanks, In *Twentieth International Workshop on Water Waves and Floating Bodies*, pp. 201–204, Oystese, Norway.

[6] Lee, Y., Tan, M., and Temarel, P. (2008), Coupling between ship motion and sloshing using potential flow analysis, In *Eighth International Conference on Hydrodynamics*, Nantes, France.

[7] McTaggart, K. (2002), Three Dimensional Ship Hydrodynamic Coefficients Using the Zero Forward Speed Green Function, (DRDC Atlantic TM 2002-059) Defence Research and Development Canada – Atlantic.

[8] McTaggart, K. (2003), Hydrodynamic Forces and Motions in the Time Domain for an Unappended Ship Hull, (DRDC Atlantic TM 2003-104) Defence Research and Development Canada – Atlantic.

[9] Molin, B., Remy, F., Rigaud, S., and de Jouette, C. (2002), LNG-FPSO's: Frequency Domain, Coupled Analysis of Support and Liquid Cargo Motions, In *International Maritime Association of the Mediterranean Conference*, Rethymnon, Greece.

[10] Nam, B.-W., Kim, Y., Kim, D.-W., and Kim, Y.-S. (2009), Experimental and Numerical Studies on Ship Motion Responses Coupled with Sloshing in Waves, *Journal of Ship Research*, 53(2), 68–82.

[11] McTaggart, K. (2004), Appendage and Viscous Forces for Ship Motions in Waves, (DRDC Atlantic TM 2004-227) Defence Research and Development Canada – Atlantic.

Symbols and Abbreviations

$[A]$	ship added mass matrix due to fluid external to ship
$[A^{slosh}]$	ship added mass matrix due to tank sloshing
$[A^{tank-fl}]$	tank total fluid added mass matrix (vertical origin at fluid line)
a	wave amplitude
B	beam
$[B]$	ship damping matrix due to fluid external to ship
$[B^{slosh}]$	ship damping matrix due to tank sloshing
$[B^{tank-fl}]$	tank fluid damping matrix for vertical origin at fluid line
$[b(U)]$	ship speed-dependent damping matrix
$[C]$	ship stiffness matrix due to fluid external to ship
C_d	hull roll drag coefficient
C_{eddy}^{hull}	hull roll eddy drag coefficient
$[C^{slosh}]$	ship stiffness matrix due to tank sloshing
CG	centre of gravity
$[c(U)]$	ship speed-dependent stiffness matrix
$\{F_D\}$	diffracted wave force vector
$\{F_I\}$	incident wave force vector
$F_4^{hull-eddy}$	hull eddy damping roll moment
$\overline{GM}$	ship metacentric height
$G(\vec{x}, \vec{x}_s)$	Green function for fluid domain location at $\vec{x}$ and source at $\vec{x}_s$
g	gravitational acceleration
H_s	significant wave height
h_{fluid}	height of fluid in sloshing tank relative to tank bottom
h_{tank}	total height of tank
$[K]$	hull retardation function matrix
$[K^{slosh}]$	sloshing retardation function matrix
k	wavenumber

L	ship length between perpendiculars
L_{tank}	longitudinal length of sloshing tank
$[M]$	ship mass matrix
$[M^{tank-fl}]$	tank fluid inertia matrix (vertical origin at tank fluid line)
m^{tank}	mass of fluid in sloshing tank
m_{44}^{tank}	roll inertia of fluid in sloshing tank
n_j^{fl}	normal component pointing into tank fluid for mode j
n_x, n_y, n_z	components of normal vector pointing into tank fluid
RAO	response amplitude operator
S_t	interior surface of sloshing tank
T	draft
T_{mid}	draft at midships
T_p	peak wave period
t	time
t_{stern}	ship trim by stern
U	forward ship speed
V_{fluid}	tank fluid volume
w_{tank}	tank width along ship lateral axis
$\vec{x}$	location in fluid domain
$\vec{x}_s$	source location
x, y, z	translating earth coordinates with origin at ship CG
x_f, y_f	earth-fixed horizontal plane coordinates
x_t, y_t	sloshing tank local horizontal plane coordinates
$\overline{x}_t^{fp}$	longitudinal centroid of sloshing tank waterplane
z_{bl}	elevation above ship baseline
z_{bl}^{tank}	elevation of tank bottom above baseline
z_{fl}	elevation above tank fluid level
β_s	relative sea direction

γ	JONSWAP spectrum peak enhancement factor
ϵ_{tank}	tank flow damping coefficient
$\hat{\epsilon}_{tank}$	peak tank flow damping coefficient
η_j	motion displacement for mode j in translating-earth coordinates
η_j^{TD}	motion displacement in time domain for mode j
$\hat{\eta}_4$	roll motion amplitude
λ_n	wavelength for natural sloshing frequency ω_n
ν	wave heading (from)
ρ_{tank}	density of fluid in sloshing tank
σ_j	source strength for ship motion mode j
τ	delay time for retardation function
τ_{max}	maximum delay time for retardation function
Φ	flow velocity potential in time domain
ϕ_j	frequency domain flow potential for mode j unit amplitude motion
χ	ship heading (to)
ω_4	ship roll natural frequency
ω_e	wave encounter frequency
ω_e^*	maximum encounter frequency for evaluation of retardation function
$\omega_{lower}^{\hat{\epsilon}}$	lower frequency for peak fluid damping
ω_n	natural sloshing frequency for sloshing mode number n
$\omega_{upper}^{\hat{\epsilon}}$	upper frequency for peak fluid damping
$\triangle$	ship mass displacement

This page intentionally left blank.

DOCUMENT CONTROL DATA

(Security markings for the title, abstract and indexing annotation must be entered when the document is Classified or Designated.)

1. ORIGINATOR (The name and address of the organization preparing the document. Organizations for whom the document was prepared, e.g. Centre sponsoring a contractor's report, or tasking agency, are entered in section 8.)

Defence Research and Development Canada – Atlantic
PO Box 1012, Dartmouth NS B2Y 3Z7, Canada

2a. SECURITY MARKING (Overall security marking of the document, including supplemental markings if applicable.)

UNCLASSIFIED

2b. CONTROLLED GOODS

(NON-CONTROLLED GOODS)
DMC A
REVIEW: GCEC JUNE 2010

3. TITLE (The complete document title as indicated on the title page. Its classification should be indicated by the appropriate abbreviation (S, C or U) in parentheses after the title.)

Modelling of Sloshing in Free Surface Tanks for ShipMo3D Ship Motion Predictions

4. AUTHORS (Last name, followed by initials – ranks, titles, etc. not to be used.)

McTaggart, K.

5. DATE OF PUBLICATION (Month and year of publication of document.)	6a. NO. OF PAGES (Total containing information. Include Annexes, Appendices, etc.)	6b. NO. OF REFS (Total cited in document.)
January 2012	56	11

7. DESCRIPTIVE NOTES (The category of the document, e.g. technical report, technical note or memorandum. If appropriate, enter the type of report, e.g. interim, progress, summary, annual or final. Give the inclusive dates when a specific reporting period is covered.)

External Client Report

8. SPONSORING ACTIVITY (The name of the department project office or laboratory sponsoring the research and development – include address.)

Canadian Coast Guard Major Crown Projects Directorate
Ottawa

9a. PROJECT OR GRANT NO. (If appropriate, the applicable research and development project or grant number under which the document was written. Please specify whether project or grant.)	9b. CONTRACT NO. (If appropriate, the applicable number under which the document was written.)
11ge01	

10a. ORIGINATOR'S DOCUMENT NUMBER (The official document number by which the document is identified by the originating activity. This number must be unique to this document.)	10b. OTHER DOCUMENT NO(s). (Any other numbers which may be assigned this document either by the originator or by the sponsor.)
DRDC Atlantic ECR 2011-084	

11. DOCUMENT AVAILABILITY (Any limitations on further dissemination of the document, other than those imposed by security classification.)

(X) Unlimited distribution
( ) Defence departments and defence contractors; further distribution only as approved
( ) Defence departments and Canadian defence contractors; further distribution only as approved
( ) Government departments and agencies; further distribution only as approved
( ) Defence departments; further distribution only as approved
( ) Other (please specify):

12. DOCUMENT ANNOUNCEMENT (Any limitation to the bibliographic announcement of this document. This will normally correspond to the Document Availability (11). However, where further distribution (beyond the audience specified in (11)) is possible, a wider announcement audience may be selected.)

13. ABSTRACT (A brief and factual summary of the document. It may also appear elsewhere in the body of the document itself. It is highly desirable that the abstract of classified documents be unclassified. Each paragraph of the abstract shall begin with an indication of the security classification of the information in the paragraph (unless the document itself is unclassified) represented as (S), (C), or (U). It is not necessary to include here abstracts in both official languages unless the text is bilingual.)

Ship roll motions in waves can be significantly influenced by the presence of tanks containing liquids, which experience sloshing. Sloshing effects must be considered when transporting liquid cargo; however, sloshing can also be used to advantage. Many vessels have specially designed flume tanks to provide passive roll stabilization. This report describes the implementation of a model of fluid sloshing in tanks for the ShipMo3D ship motion library. The sloshing model is based on potential flow, giving a solution that is computationally efficient and robust. The potential flow model includes a simplified treatment of flow damping arising from viscous effects. The tank sloshing model has been implemented for computations in both the frequency and time domains. Example computations for a generic frigate demonstrate the reduction of roll motions using a flume tank.

14. KEYWORDS, DESCRIPTORS or IDENTIFIERS (Technically meaningful terms or short phrases that characterize a document and could be helpful in cataloguing the document. They should be selected so that no security classification is required. Identifiers, such as equipment model designation, trade name, military project code name, geographic location may also be included. If possible keywords should be selected from a published thesaurus. e.g. Thesaurus of Engineering and Scientific Terms (TEST) and that thesaurus identified. If it is not possible to select indexing terms which are Unclassified, the classification of each should be indicated as with the title.)

frequency domain
roll
ship motions
simulation
sloshing
time domain
waves